

1 **Knickpoints and Fixpoints: The Evolution of Fluvial Morphology** 2 **under the Combined Effect of Fault Uplift and Dam Obstruction on a** 3 **Soft Bedrock River**

4 Hung-En Chen¹, Yen-Yu Chiu^{1,2}, Chih-Yuan Cheng¹ and Su-Chin Chen^{1,3}

5 ¹ Department of Soil and Water Conservation, National Chung Hsing University, Taichung 40227, Taiwan

6 ² [Department of Geography, National Changhua University of Education, Changhua 50074, Taiwan](#)

7

8 ³ Innovation and Development Center of Sustainable Agriculture, National Chung Hsing University, Taichung 40227, Taiwan

9 *Correspondence to:* Su-Chin Chen (scchen@nchu.edu.tw)

10 **Abstract.** Rapid changes in river geomorphology can occur after being disturbed by external factors like earthquakes or large
11 dam obstructions. Studies documenting the evolution of river morphology under such conditions have advanced our
12 understanding of fluvial geomorphology. The Dajia River in Taiwan presents a unique example of the combined effects of a
13 coseismic fault (the 1999 Mw 7.6 Chi-Chi earthquake) and a dam. As a result of the steep terrain and abundant precipitation,
14 rivers in Taiwan have exhibited characteristic post-disturbance evolution over 20 years. This study also considers two other
15 comparative rivers with similar congenital conditions: the Daan River was affected by a thrust fault Chi-Chi earthquake, too;
16 the Zhuoshui River was influenced by dam construction finished in 2001. The survey data and knickpoint migration model
17 were used to analyze the evolution of the three rivers and propose hypothesis models. Results showed that the mobile
18 knickpoint migrated upstream under the influence of flow, while the dam acted as a fixpoint, leading to an increased elevation
19 gap and downstream channel incision. Thereby, the Dajia River narrowing and incision began at both ends and progressively
20 spread to the whole reach under the combined effects.

21 **KEYWORDS:** dam obstruction; fixpoint; coseismic uplift; knickpoint; soft bedrock incision; river evolution

22 1. Introduction

23 Natural tectonic movements and artificial structures are the main factors that disturb river **sediment equilibrium** (Whipple
24 **and Trucker, 2002; Lang et al., 2003; Dotterweich, 2008; Cook et al., 2013; Hoffmann, 2015**). These external influences often
25 interact complexly; therefore, distinguishing between anthropogenic and natural drivers of landscape evolution is difficult. In
26 addition, changes in these external conditions, in turn drive adjustments in the riverbed, generating new landscape patterns.
27 River morphological development generally reflects the geology and flow stress conditions (Lyell, 1830). When a **significant**
28 **substantial** external impact occurs, a knickpoint (a localized discontinuity in the longitudinal profile of the riverbed) often
29 forms (Holland, 1976), **varying in size from a single waterfall to stretches spanning several kilometers (Holland, 1976; Crosby**
30 **and Whipple, 2006)**. These features may develop due to natural events such as **Knickpoints can range in scale from a single**
31 **waterfall to a zone of several kilometers (Crosby and Whipple, 2006) and may result from natural factors such as extreme**
32 **weather, sea-level fall, and earthquake-induced surface rupture (Seidl and Dietrich, 1992; Whipple, 2004; Bishop et al., 2005;**
33 **Heijnen et al., 2020).**

34 The active fault causes a prominent knickpoint in a stream, known as tectonic uplift, leading to a local increase in channel
35 steepness (Hayakawa et al., 2009; Huang et al., 2013; Cook et al., 2013). The **abrupt sudden** elevation change in the riverbed
36 divides the river profile into two reaches with differing slopes, altering the base level of fluvial erosion. The increasing flow
37 stress erodes the knickpoints, causing it to migrate upstream-ward over time. **A long duration is required for the fluvial response**
38 **to adapt to localized surface uplift or depositional blockage by knickpoint retreat and migration upstream with time, cutting a**
39 **narrow channel and even forming a canyon.** The migration process and speed are highly variable and depend on the tectonic
40 **setting** and physical nature of the riverbed (Whipple and Trucker, 2002; Whipple et al., 2004). **However, the fluvial response**
41 **to knickpoint retreat and upstream migration requires a long duration (Howard et al., 1994; Tomkin et al., 2003), often**
42 **accompanied by the cutting of a narrow channel and even the formation of a canyon. Therefore, extensive studies have been**
43 **attracted and tended to explore the formation and migration of knickpoints due to increases in elevation and relief. The**
44 **emergence and migration of knickpoints caused by disturbance from external conditions was studied extensively (Whipple,**
45 **2001; Whipple and Trucker, 2002; Crosby and Whipple, 2006; Clark, 2014; Ahmed et al., 2018).**

46 Anthropogenic factors, such as reservoir construction, which is one of the most common ways humans interfere with river
47 hydrology and sedimentation (Magilligan and Nislow, 2005; Petts and Gurnell, 2005; Graf, 2006; Nelson et al., 2013; Liro,
48 2017, 2019; Zhou et al., 2018). Dam as a fixpoint in the river influences two critical components of river geomorphology: the

49 sediment transport capacity of the flow and the oncoming sediment load (Williams and Wolman, 1984). ~~If the sediment~~
50 ~~transport capacity exceeds the oncoming sediment load, the amount of sediment may be insufficient to maintain the riverbed~~
51 ~~level, and erosion may occur. Conversely, if the sediment load exceeds the sediment transport capacity, deposition on the~~
52 ~~riverbed would be expected to occur.~~ The self-adjustment mechanisms of river channels responding to insufficient or excess
53 sediment (Brandt, 2000) ~~result~~ results in the change in cross-section geometry, bed material size, river pattern (Leopold and
54 Wolman 1957), and slope. Previous studies on the evolution of areas downstream of dams have primarily analyzed changes in
55 downstream sandbars over large spatial scales (Horn et al., 2012; Słowik et al., 2018; Kong et al., 2020) or the ecology of the
56 lower reaches in front of dams (Kingsford, 2000; Braatne et al., 2008; Shafroth et al., 2016). Few studies of exposed bedrock
57 have been based on long-term observations (Inbar, 1990). In most cases, a dam effectively traps the sediment supply from the
58 watershed. If sediment transfer to the downstream reaches of the dam is reduced, the armor layers of the riverbed are lost,
59 which may cause an incision of the fluvial channel (Surian and Rindai, 2003). This incision subsequently narrows the river
60 cross-sections and lowers the thalweg level.

61 Decades or hundreds of years are generally required for a riverbed to reach a new equilibrium after disturbance by external
62 conditions, so it is difficult to understand such changes based on short-period observational data (Howard et al., 1994; Tomkin
63 et al., 2003). Because of the abundant rainfall brought by typhoons and monsoons, the river terrain in Taiwan can alter
64 dramatically over a short period of time. Moreover, dams in Taiwan are built primarily in steep reaches, enhancing the rapid,
65 remarkable morphological evolution of the downstream reaches. ~~The reservoirs of dams constructed on the rivers become~~
66 ~~silted up, resulting in a lack of sediment downstream in the meantime, which causes loss of armor layers, exposure of soft rock,~~
67 ~~and severe erosion. Another factor influencing the distinctive characteristics of Taiwanese rivers is the geological location;~~
68 ~~Taiwan is located in a plate junction zone that experiences frequent earthquakes such as t~~The Chi-Chi Earthquake ~~of in~~ 1999
69 ~~(Lin et al., 2001; Ota et al., 2005), which~~ caused the offset of the Chelungpu thrust fault in central Taiwan (Lin et al., 2001;
70 Ota et al., 2005). The surface rupture and uplift induced the formation of knickpoints and river gorges. Twenty years later, the
71 undercutting trend of the active channel below dams and the migration of post-earthquake knickpoints have caused the rivers
72 to evolve into their present forms. This rapid evolution of river morphology over a short time makes Taiwan rivers suitable as
73 case studies. The Dajia River is a unique example, as a dam structure and coseismic uplift impact it simultaneously in a short
74 reach. The current work aims to clarify the river changes caused by the earthquake and a dam, and to propose a hypothesis for
75 the evolution model. To compare the various morphological developments under different external conditions, the Daan,

76 Zhuoshui, and Dajia rivers in central Taiwan are considered in this study.

77 2. Study area, materials, and methods

78 The longitudinal changes of the river bed and the accompanying river pattern changes are the objects of observation. A
79 common type of longitudinal profile development for knickpoint retreat is illustrated in Fig. 1a (Gardner, 1983; Whipple and
80 Trucker, 1999; Crosby and Whipple, 2006; Parker and Izumi 2000; Alonso et al. 2002; Bressan et al., 2014). As the base level
81 of erosion fell, the stream encountered an abrupt shift in slope from gentle to steep, which significantly accelerated the flow
82 and subsequently led to stream bed erosion. During this process, apparent upstream degradation and downstream aggradation
83 occurred. The knickpoint migrated upward with time, accompanied by slope replacement. After the river had reached a new
84 equilibrium in a channelized pattern, the slope replacement resulted in a natural profile. During the adjustment, the incision
85 trend gradually slowed, and sedimentation may commence downstream (dashed line in Fig. 1a). The profile evolved from a
86 concave curve to a graded profile (Chamberlin and Salisbury, 1904). The well-known result of dam construction is the
87 progressive loss of the armor layer in the neighboring downstream river (Fig. 1b). The scouring baseline extended downstream-
88 ward from the dam (Olsen, 1999; Choi et al., 2005; Słowik et al., 2018). Because of the fixpoint, the local slope at the dam toe
89 became steeper progressively, and the dam caused the downstream river profile to be gentle and sediment transport to decrease.

90 ~~However, significant changes in the longitudinal profile must also be accompanied by variations in river patterns, which~~
91 ~~have yet to receive much attention. Furthermore, and,~~ the interaction between fault scarps and dam obstructions within a river
92 reach is rarely observed and studied. To address the morphological developments under different external conditions ~~se gaps,~~

93 we collected historical data (incl. multiyear satellite images, orthographic images, cross-sectional and longitudinal profiles.)
94 for three rivers in Taiwan (Daan, Zhuoshui, and Dajia), each representing the individual effects of faults and dams, as well as
95 their combined effects.

96 2.1 Study area

97 Taiwan's climate is strongly affected by the western Pacific tropical cyclone. There are approximately three to four
98 typhoons and heavy rain events yearly, and the average annual precipitation is about 2500 mm. The heavy rains during the
99 monsoons and typhoons cause dramatic changes to riverbeds over short periods of time. In addition, because Taiwan is located
100 at the compressive tectonic boundary between the Eurasian and Philippine Sea plates, the collision of the two continental plates
101 causes tectonic breakage of the strata. On September 21, 1999, the Chi-Chi earthquake ($M_w = 7.6$) resulted in uneven uplift in
102 the island. Three central Taiwan rivers illustrate dams or faults' effects (Figure 2): The Daan River has been affected by vertical

103 fault scarps, the Dajia River by both fault scarps and a dam, and the Zhuoshui River by dam obstruction. These three important
104 rivers have very similar characteristics: their east-to-west flow direction; their range of elevation from sea level to ~3000 m;
105 their steep river slopes (the average slope of each river 1.5% – 2.4%, Kuo et al.(2021)); and the presence of soft rock in the
106 mid-stream (as shown in the pink region in Fig. 2). The locations of the three rivers and the Chelungpu thrust fault are marked
107 in Fig. 2. The southern termination of the fault crosses the Zhoushui River trending ~~north-south~~north-south; the northern
108 termination near the Dajia and the Daan rivers shows a complex deformation pattern trending NE–SW to E–W (Lee et al.,
109 2002), composed of several parallel thrust faults. In the three studied reaches, the Pleistocene sedimentary rocks are mainly
110 composed of soft rocks consisting of sandstone, siltstone, shale, and mudstone. Soft rocks have intermediate strength between
111 soils and hard rocks, ~~possessing with possessing~~ unconfined compressive strengths ranging from 0.5 to 25.0 MPa (Lai et al.,
112 2011). These rocks are generally poorly lithified and weakened by a high water content; therefore, their resistance to water
113 erosion is poor. The riverbed rock is readily incised by flooding flow when the upper armoring protective layer was lost (Huang
114 et al., 2014).

115 The Chi-Chi earthquake produced a surface rupture 80 km long. Several fracture planes at the north end of the fault
116 caused uneven uplift in the region (Lee et al., 2002). One of the ruptures passed through the right bank of the Shigang Dam
117 (constructed in 1977) on the Dajia River, causing serious damage to the dam structure. The maximum vertical displacement of
118 the surface rupture was 9 m, increasing the drop height of the bed level between the face and the back of the dam markedly.
119 The dam reconstruction was finished in 2000. The repaired Shigang Dam was intended to store 2.4×10^6 m³ of water after the
120 Chi-Chi earthquake; however, owing to deposition in the reservoir, only $\sim 1.4 \times 10^6$ m³ of water can now be retained. After the
121 earthquake and the reconstruction, the fluvial morphology has been changed rapidly. The original armor layers on the riverbed
122 in front of the Shigang Dam were lost rapidly, ~~exposing the soft bedrock~~and the soft bedrock was exposed. The two rupture
123 surfaces at the north end of the Chelungpu Fault uplifted a 1 km reach of bed in the Daan River, with a maximum vertical
124 uplift of 10 m.

125 Although the southern end of the Chelungpu Fault passes downstream of the Jiji Dam (Zhuoshui River), the fault uplifted
126 the bed level by ~2 m, less than the uplifts in the Daan and Dajia rivers. The Jiji Dam was built in 2001 (after the 1999 Chi-
127 Chi earthquake), is situated on the narrowest part of the Zhuoshui River, and has a maximum designed storage capacity of 10
128 $\times 10^6$ m³. Due to the large sediment yield in the Zhuoshui River watershed, the present-day adequate water storage capacity is
129 only $\sim 4 \times 10^6$ m³. The Jiji Dam downstream is known for its soft bedrock canyon features, formed by dam-obstructed water

130 scouring.

131 2.2 Data Collection and Analysis MethodsMaterials

132 Analysis of the effects of faults and dams, alteration of river patterns, changes in thalweg levels, and variations in river
133 cross-sections are crucial to revealing the process of river evolution. SPOT-5 and SPOT-6 satellite images (2 m in
134 resolutions) and orthographic images (25 – 50 m in resolutions) obtained by the Center for Space and Remote Sensing
135 Research, National Central University (CSRSR/NCU) and the Aerial Survey Office (AFASI) of Taiwan were used to
136 assess changes in river patterns. Multiyear cross-sectional and longitudinal profiles were established from historical
137 surveys by the Water Resources Agency (WRA). The survey was conducted using Total Station, GPS, and depth sounder.
138 The interval of survey points should be 5–10 m, and the elevation error must not exceed cm. Additional analyses of
139 knickpoint retreat and variations in river elevation and width were carried out. We also incorporated terrain data from
140 other relevant studies into our research materials. For example, the longitudinal profiles proposed by Cook et al. (2013),
141 which generated Digital Surface Models (DSMs) for the years 1998 and 2004 using aerial photographs, were also
142 included in our research materials. The locations of knickpoints were determined by identifying abrupt terrain changes
143 and the positions of splash in the images. We also collected the daily flow data from the WRA and calculated the
144 cumulative flow to compare the relationship between knickpoint retreat and discharge. The widthWidth (W) and depth
145 (D) of the river can be used to quantify changes in river patterns. In order to analyze the variation of channel width-~~(W)~~,
146 depth-~~(D)~~, and aspect ratio (W/D), we calculated the bank-full discharge width and depth, which represents the maximum
147 flow that can occur in a river before water starts overflowing and spreading out onto the floodplain. We identified the
148 river banks and extracted channel widths from orthographic images. The banks were defined as the boundaries between
149 the main channel and the adjacent floodplain.

150 2.3 Mathematical model

151 The application of the mathematical model provides an abstract description of a concrete system using physical concepts
152 and mathematical language. A one-dimensional Exner equation (Exner, 1925) is used to describe the advective and diffusive
153 knickpoint migration (Bressan et al., 2014):

$$154 \quad \frac{\partial z}{\partial t} + \frac{1}{(1-p_s)} \frac{\partial q_s}{\partial x} = 0 \quad (1a)$$

155 where z is the bed elevation along the thalweg, p_s is the porosity of bed sediment, t is the time, x is the distance, and q_s is
156 the sediment discharge per unit width that is estimated by the product of the surface height change η , and the knickpoint

157 migration rate dx/dt is expressed as equation 1b.

$$158 \quad q_s = -\eta \frac{dx}{dt} \quad (1b)$$

159 The migration rate as a sediment separation per unit area homogeneously distributed over the eroding surface is expressed
160 as equation (1c).

$$161 \quad \frac{dx}{dt} = k_d[\tau(x) - \tau_c] \quad (1c)$$

162 where k_d is the erodibility, τ is the bed shear stress, and τ_c is the critical shear stress of the bed material. The condition of
163 an obvious knickpoint face, τ should be estimated using a formula that considers knickpoint as a submerged obstacle
164 (equation (1d)) (Engelund, 1970).

$$165 \quad \tau(x) = M\tau_0 \left[1 + A \frac{(z-z_0)}{H_0} + B \frac{\partial z}{\partial x} \right] \quad (1d)$$

166 The factors M , A , and B in equation (1d) are parameters related to localized phenomena. τ_0 , z_0 , and H_0 are the shear
167 stress, bed elevation and the water depth upstream of the knickpoint. The term $B \frac{\partial z}{\partial x}$ represents the change in shear stress due
168 to the local slope. The shear stress in the channel section upstream of the knickpoint crest ($\tau_0 = \gamma H_0 S_0$, where γ is the specific
169 weight of water changes across the knickpoint due to the abrupt change in bed topography (equation (1d)). Substituting
170 equations (1b)–(1d) into equation (1a), equations (2a)–(2c) were obtained in below:

$$171 \quad \frac{\partial z}{\partial t} - C \frac{\partial z}{\partial x} - D \frac{\partial^2 z}{\partial x^2} = 0 \quad (2a)$$

$$172 \quad C = \left(\frac{\eta k_d \gamma}{1-p_s} \right) S_0 M A \quad (2b)$$

$$173 \quad D = \left(\frac{\eta k_d \gamma}{1-p_s} \right) S_0 H_0 M B \quad (2c)$$

174 where the coefficients of the first- and second-order spatial derivatives, C and D , are known as the advection and diffusion
175 coefficients, respectively. [C represents the moving speed, and D represents the diffusion constant.](#) It can be concluded that the
176 key controls of the knickpoint retreat are the channel slope, the erodibility of the bed of the river reach, the knickpoint face
177 height, and the upstream water depth. [The survey data could calibrate these physical parameters](#) ~~These physical parameters~~
178 ~~could be calibrated by the survey data.~~ –Therefore, the present equation is a physical-based model that can be solved with the
179 second-order accurate implicit finite difference scheme which was implemented in MATLAB. However, it is essential to
180 recognize that the numerical model is conceptual and involves several assumptions, such as not considering variations in the
181 horizontal 2D plane of the terrain and assuming homogeneous parameters within the simulation area, among others. The
182 numerical model cannot fully capture the ~~actual~~ scenario's detailed morphology and environmental conditions; it ~~is serves as~~ a
183 conceptual model based on physical mechanisms, providing trends rather than precise representations.

184 3. RESULTS

185 3.1 Fault effect on Daan River canyon

186 The scarps across the Daan River that were uplifted by the Chi-Chi earthquake caused a dramatic change in the topography,
187 disturbing the dynamic equilibrium of the fluvial system. Cook et al. (2013) proposed that the knickpoint propagated rapidly
188 after 2004 and pointed out that the tool effect caused pronounced fluvial incision of the bedrock after the disappearance of
189 bedload. Knickpoint propagation was influenced by the antiformal geological structure of the area, the presence and orientation
190 of interbedded strong and weak lithologies, and the proportion of discharge entering the main channel. Huang et al. (2013)
191 also proposed that the knickpoint retreat rate can be affected by several factors, including discharge, rock properties, geological
192 structures, and bedrock orientation. The channel development of the studied reach and the behavior of knickpoint retreat were
193 assessed by analyzing multiyear data on the form and cross-section of the river.

194 Successive orthographic images of the studied reach of the Daan River from 2000 to 2017 and the corresponding flow
195 paths are illustrated in Fig. 3. River cross-sections constructed from precise survey data are provided in Fig. 4. Chronological
196 longitudinal profiles of the river reach are shown in Fig. 5. Longitudinal profile data from Cook et al. (2013) were included to
197 make information more complete. The effect of the earthquake on the surface elevation is clearly visible in Fig. 5. In addition
198 to the survey data, the advective and diffusive knickpoint migration model (equation 2) was solved to mathematize the
199 knickpoint retreat progress after the Chi-Chi earthquake. The initial condition and boundaries condition are needed to solve
200 the equation. The initial condition is the longitudinal profile in 1999, while the boundary conditions are the real bed changes
201 in upstream and downstream boundaries. The C and D are physical parameters and were calibrated by the survey data. In
202 equation 2, C represents the moving speed, and D represents the diffusion constant. These two coefficients reflect the rate of
203 bed erosion, which is physically composed mainly of bed shear stress (equations 2b and 2c). Due to the actual bed erosion
204 rates varying with time, the parameters were adjusted to match the real changes. Before 2004, C was 22.0 m/yr, and D was
205 10.0 m²/yr; after 2004, C was 91.5 m/yr, and D was 18.5 m²/yr, and the simulation was continued until 2011 when the
206 knickpoint ~~disappeared~~disappear. The result of the modeling is shown at the top left corner in Fig. 5. The knickpoint
207 progressively retreats, accompanying by slope replacement. The variation trend of the simulation and survey data is generally
208 consistent, and the speed (C) has a larger value in 2004 – 2011, which is also consistent with the observation.

209 The long-term development of the studied reach of the Daan River in the past 20 years, after the coseismic uplift, can be
210 divided into three periods: downstream erosion and slow knickpoint migration (earthquake to 2004); sudden migration of the

211 knickpoint (2004 – 2011); and gorge widening and eradication (2011 – present).

212 **3.1.1 Downstream erosion and slow knickpoint migration (earthquake to 2004)**

213 After the Chi-Chi earthquake, coseismic ground deformation created a pop-up obstruction across the river, forming a
214 barrier lake behind the rupture scarp. The obstacle blocked the river flow and trapped the sediment, causing the river bed
215 downstream of the rupture scarp completely lose the armor layer. When the armor layer was lost, bedrock incision occurred
216 downstream of the uplifted zone, and the knickpoint retreat appeared. On the other hand, no significant erosion occurred
217 between cross-sections **a** and **b** during that period (Figs 3 and 4). A comparison of the cross-sections for 2000 and 2004 (Fig.
218 4) reveals that most parts of the section **a** even experienced deposition. Slight erosion in some places can be detected in the
219 longitudinal profiles (Fig. 5) between 1999 (after the earthquake) and 2004. Although the seismic uplift produced an obvious
220 knickpoint on the riverbed, that knickpoint migrated only slightly (85 m; Table 1) between 2000 and 2004. The downstream
221 reach of the uplifted zone showed evidence of scour, but no noticeable bedrock incision or canyon landscape had developed
222 yet.

223 **3.1.2 Sudden migration of knickpoint (2004–2011)**

224 The orthographic image for 2007 (Fig. 3) clearly shows that the armor layer had been removed, the bedrock had been
225 exposed, and the deep incision had formed a narrow channel. The knickpoint retreated upstream-ward by approximately 422
226 m between 2004 and 2007, accompanied by continued scouring downstream. In the uplifted reach, under the stress of the
227 concentrated flow in the newly formed channel, the tool effect resulted in a deepened incision of the rock bed, and a canyon
228 landform gradually developed. In the 2007 cross-section data for section **a**, a canyon close to the left bank can be observed,
229 which persisted until 2011. A rapid incision rate (5.6 m/yr) occurred in section **a**, which also experienced a narrowing rate of
230 about 105.5 m/yr. Bed incision and narrowing of the main channel occurred in section **b** simultaneously, with a narrowing rate
231 of approximately 89.9 m/yr and an incision rate of about 2.1 m/yr. Between 2007 and 2011, the knickpoint retreated upstream
232 by about 412 m; the incision at section **a** was lessened, but section **b** experienced a notable incision into the rock bed
233 accompanied by knickpoint retreat. Because an obvious gorge channel had appeared in the uplifted zone, sediment from
234 upstream was transported downstream, and downstream scouring transformed gradually into sedimentation; therefore, the
235 convex longitudinal profile was gradually erased.

236 **3.1.3 Gorge widening and eradication (2011 to the present)**

237 After 2011, the knickpoint became insignificant in the longitudinal profile, so the thalweg scouring trend slowed. The

238 morphology development is dominated by lateral erosion instead of vertical incision. The narrow, deep canyon evolved into a
239 U-shaped canyon with a wide bottom. River pattern migration from upstream caused the canyon-type channel to commence
240 transforming into a braided channel. The main channel of section **a** experienced deposition as a result of the sediment supply
241 being adequate (Fig. 5). Cook et al. (2014) proposed a mechanism of gorge eradication, called *downstream sweep erosion*,
242 which rapidly transformed the gorge into a beveled floodplain through the downstream propagation of a wide erosion front
243 located where the broad upstream channel abruptly became a narrow gorge. The sweep boundary is clearly visible in the
244 orthographic images for 2011 and 2017 (Fig. 3). Additional large floods are expected to cause a marked widening of the channel
245 instead of deepening (Huang et al., 2013). It has been estimated that removal of the gorge erosion will take 50 years (Cook et
246 al., 2014).

247 Significant incision of the channel is common after a riverbed has been uplifted suddenly by tectonic movement and the
248 bed slope changes dramatically (Merritts et al., 1989). This was the case for the Daan River after the Chi-Chi earthquake. After
249 the coseismic uplift, the base level of erosion downstream reduced, so erosion increased. The river width became notably
250 narrower and deeper. Upward movement of the knickpoint caused the river channel in the uplifted section to narrow rapidly.
251 The concentrated flow caused a rapid incision of a weak geological layer in the riverbed, so the channel width decreased
252 sharply. Therefore, the uplifted section formed a canyon landform. As the slope at the knickpoint gradually recovered, the
253 incision slowed and sediment transport down the recovered river resulted in sediment deposition in the downstream channel.
254 The river also gradually developed lateral erosion upstream, and the river channel tended to widen. The channelization is
255 expected to have been swept because the sweep boundary migrated progressively downward.

256 **3.2 Jiji Dam effect on Zhoushui River**

257 Construction of the Jiji Dam on the Zhoushui River began in 1996 and operated in 2001. Orthographic images, flow paths
258 of the studied reach, and the locations of cross-sections **c**, **d**, and **e** below the Jiji Dam for 1998 to 2018 are provided in Fig. 6.
259 Chronological survey data of cross-sections **c**, **d**, and **e** are provided in Fig. 7. Chronological longitudinal profiles of the studied
260 reach are illustrated in Fig. 8. The river is located at the southern termination of the Chelungpu Fault (Fig. 1), where the
261 elevation gap caused by the earthquake is relatively small. In 1998, the Zhoushui River was a broad braided river, with many
262 sandbars downstream of the dam (Fig. 6). In 2003, two years after dam operation had commenced, the riverbed armor layer
263 had been lost and the exposed soft bedrock was clearly visible within 700 m of the toe of the dam, because of a lack of sediment.
264 The bedrock's incision deepened due to the tool effect, and the flow path concentrated gradually in front of the dam. From

265 2003 to 2007, the effect zone gradually expanded, and exposed bedrock extended to ~3.2 km downstream from the dam.
266 Between 2007 and 2018, the channelization and the zone with exposed bedrock expanded continuously to 6.5 km downstream
267 of the dam. Due to the channelization, the river cross-section became narrow and deep.

268 The transformation of the river and the rates of lateral and vertical change are clearly visible in the river cross-sections
269 (Fig. 7). There was no apparent erosion of section **c** in 2008, but the sections closer to the dam (**d** and **e**) exhibited obvious
270 incision (Fig. 7). After the loss of the riverbed armor layer, the flow cut down into weak bedrock. The deep main channels'
271 development is clearly visible in sections **d** and **e** between 1998 and 2008. During this time, the incision rate of section **e** was
272 around 1.2 m/yr, and the narrowing rate was around 25 m/yr. During 2008 – 2012, engineering measures were installed:
273 between section **d** and section **e**, groundsills, spur dikes and tetrapod were added to the river channel to prevent erosion, and
274 the riverbed level rose slightly at section **e**. However, the channel width of section **c** was markedly narrower, with a narrowing
275 rate of roughly 65 m/yr. Between 2008 and 2015, ~~the incision rates of~~ sections **c** and **d** incision rates were roughly 1.4 m/yr.
276 Progressive erosion layer by layer is apparent in the chronological longitudinal profiles (Fig. 8). Incision of the studied reach
277 became increasingly severe: incision commenced at section **e** and subsequently extended downstream to sections **d** and **c**. We
278 infer that headward erosion did not dominate the riverbed because the Chelungpu Fault passed through the river some distance
279 from the dam and caused only 2 m of uplift; on the contrary, dam-induced downward incision of the riverbed caused
280 degradation of the reach. There is an approximately 15 m difference between the bed level of 1998 and that of 2018.

281 3.3 The combined effect of Shigang Dam and Fault on Dajia River

282 The studied reach of the Dajia River, which lies downstream of the Shigang Dam, was affected by both the dam and uplift
283 caused by the Chi-Chi earthquake. The Shigang Dam was broken by uneven uplift of the fault scarp across the dam (9 m on
284 the right side and 3 m on the left), and the downstream section **f** rose by ~7 m (see Fig. 2). The earliest knickpoint formed close
285 to section **f** and moving headward with time. During 2000–2005, the knickpoint retreated by ~40 m, and another new
286 knickpoint formed between sections **g** and **h** (Fig. 9) under the co-effect of river pattern changes and bed rock differential
287 erosion. The damming effect of the Shigang Dam also caused the armor layer to be removed. The bedrock became exposed
288 shortly after the earthquake; however, section **f** was obviously incised during 2000–2005, whereas incision of section **g** did not
289 occur until 2005–2008 (Fig. 10). Between 2000 and 2005, engineering measures were installed on several occasions to mitigate
290 the obvious erosion. The river pattern between section **g** and the dam was a braided river during the period.

291 The incision rate of section **g** was ~ 1.1 m/yr during 2005–2008, and the narrowing rate was ~ 47.7 m/yr. During the same
292 time interval, the downstream knickpoint (between sections **f** and **g**) disappeared due to river training in 2008. The knickpoint
293 between section **g** and section **h** retreated rapidly toward the dam (Figs 9, 11). During 2005–2008 and 2008–2017, the
294 knickpoint moved upstream by approximately 186 and 219 m, respectively. This retreat of the knickpoint implies that river
295 channel scouring did not stop. Because the riverbed strata trend ~~northeast-southwest~~northeast-southwest, flow scouring
296 preferentially deepened the left part of the rock bed, which moved the channel closer to the left bank. After 2008, the flow
297 channel extended closer to the toe of the dam. Due to the severe incision, the government started surveying section **h** after
298 2010 (Fig. 10). Significant bedrock incision was recorded, with an incision rate of ~ 1.4 m/yr at section **h** during 2010–2017.
299 In 2008, it can be observed that the knickpoint existed in the reach between sections **g** and **h**; therefore the slope of the channel
300 is still discontinuous. The 2017 photograph shows a single, meandering channel that starts from the dam and runs through
301 sections **h** and **g**, eventually reaching section **f**, where the knickpoint had initially formed (Fig. 10). Overall, the area
302 downstream of the Shigang Dam displayed headward erosion of the knickpoint and incision of the rock bed in front of the
303 dam.

304 In the Dajia River, the advection and diffusion equation (equation 2) was also used to represent the variation mode of
305 knickpoint and bed elevation. The initial condition is the longitudinal profile in 2000. The coefficients C and D were influenced
306 by bed shear stress. Due to the rapid increase in actual bed erosion rate after 2005, the parameters were adjusted to match the
307 actual changes. Before 2005, C was 7.5 m/yr, and D was 1.825 m²/yr; after 2005, C was 36.5 m/yr, and D was 9.125 m²/yr,
308 and the simulation was continued until 2017. The downstream boundary adopts the real bed change, while the upstream
309 boundary condition is fixed, considering the dam is a fixed point. The bed is progressively scoured in the nearby downstream
310 of the dam, and the knickpoint retreats and gradually fades away. The variation trend of the simulation and survey is generally
311 consistent, excluding the fact that intensive engineering works have been conducted in front of the dam to stabilize the bed.

312 4. Discussion

313 Data on the changes in the riverbed, river width, and migration distance of the knickpoint for all three studied reaches are
314 provided in Table 1. Also, in Fig. 12(a), We use “T” symbols to represent the channel width (W) and depth (D) of the cross-
315 sections in three study reaches. The aspect ratio (W/D) is labeled above every “T.” After the Chi-Chi earthquake, the channel
316 geometry was not disturbed immediately. The aspect ratio of the Daan River exhibited only slight changes. Consequently, the
317 aspect ratio significantly decreased with time from the downstream section; subsequently, the aspect ratio recovered a little

318 after 2011. The deepening of the upstream was slower than that downstream, but the later recovery was more obvious in the
319 upstream area. The aspect ratio of the Zhuoshui River dramatically declined in the upstream part after construction of the Jiji
320 Dam; this change extended gradually to the downstream section with time. In the Dajia River, owing to the combined effects
321 of the upstream dam and the earthquake, channelization of the river started at both ends of the reach and then met in the middle.
322 The examples of these three rivers allow us to deduce the evolution of knickpoint retreat and transformation of the river pattern
323 under the influence of dams and/or uplift.

324 The river pattern of knickpoint retreat is illustrated in Fig. 12(b), and it was also observed in the Daan River. During the
325 knickpoint retreat, the tool effect caused the river to narrow dramatically. However, after the river had reached a new
326 equilibrium in a channelized pattern, the slope replacement resulted in a natural profile. The incision trend gradually slowed
327 during the adjustment, and sedimentation may commence downstream (dashed line in Fig. 12(b)). The profile evolved from a
328 concave curve to a graded profile (Chamberlin and Salisbury, 1904). In the case of the Daan River, the topography of the
329 upstream gorge was gradually swept away, and the river pattern may be slowly restored to the original braided plain.

330 Before construction of the Jiji Dam, the studied reach of the Zhoushui River was a broad braided river. The river armor
331 layer was lost due to sediment trapping by the dam. Under the influence of the tool effect, the flow path in front of the dam
332 gradually narrowed (Fig. 12(c)). The scouring boundary extended downstream-ward from the dam. Because of the immovable
333 knickpoint, the local slope at the dam toe became steeper, and the dam (acting as a non-erasable knickpoint) caused the river
334 profile and sediment transport to remain non-equilibrium.

335 The reach downstream of the Shigang Dam on the Dajia River was simultaneously affected by coseismic uplift and the
336 incision of a deep path in the soft rock in front of the dam. The knickpoint caused by fault uplift retreated upward with time.
337 Although the uplift of the Dajia River was similar to that of the Daan River, the Shigang Dam (fixpoint) restricted knickpoint
338 retreatment in the Dajia River, and led to scouring downward from the dam site. Therefore, we saw the river narrowing at the
339 two ends of the affected reach, then progressively extending to the middle, as shown in Fig. 12(d). The knickpoint caused by
340 the earthquake was gradually removed, but the effect of the dam remains. Therefore, the recovery of start of recovery to a
341 braided river cannot happen in the Dajia River.

342 In Fig 13, the discharge data of outflow from Shigang Dam (Dajia River) and Jiji Dam (Zhuoshui River), as well as and
343 the flow data of the Daan River from July 2005 to December 2019, are presented. The cumulative flow results show that the
344 increasing trends of the discharge in the Dajia and Zhuoshui Rivers are consistent. Both dams serve the purpose of controlling

345 water levels for water supply and irrigation. The direct discharge is influenced by the variations in dry and rainy seasons,
346 resulting in intermittent changes in the discharge. In contrast, the flow in the Daan River shows ~~continuous~~ ~~continuously~~ and
347 ~~stable~~ ~~increase~~ ~~increasing~~. We observed a positive correlation between the knickpoints retreat distances and the cumulative
348 discharge in the Dajia River and also in ~~the~~ Daan River. ~~However, the proportionality between discharge and knickpoint retreat~~
349 ~~rate in each river cannot be directly applied to another river (as evidenced by the comparison between the Dajia River and the~~
350 ~~Daan Rivers~~ ~~River~~). We speculate that this may be related to factors such as slope, river width, the elevation difference between
351 ~~the two river sections being a fixed point and a moving point, the protective engineering works under the Shigang Dam of the~~
352 ~~Dajia River, and local geology, among others.~~ ~~However, the correlation between flow and retreat distance does not exist when~~
353 ~~comparing different rivers. Additionally, A relationship between discharge and the changes in channel widening or the incision~~
354 ~~depth cannot be found.~~

355 Overall, there are apparent differences in the morphological changes to rivers caused by natural and human factors. A
356 knickpoint formed by fault-induced riverbed uplift is a moving point: as the knickpoint moves, the riverbed evolves gradually
357 from an unstable state to an equilibrium. In contrast, a dam can be regarded as a fixpoint on the river. The flow from the
358 spillway outlet hits the riverbed continuously, ~~which causes,~~ ~~resulting in~~ a decline of the erosion base level; therefore,
359 downward erosion commences from the toe of the dam. For the case under the combined effect of fault uplift and dam
360 obstruction, we inferred a schematic diagram of longitudinal profile development for the combined effects as shown in Fig.
361 14. In Fig 14, the uplift creates knickpoints that gradually retreat upstream. Meanwhile, ~~starting~~ ~~Starting~~ from the dam toe,
362 ~~there is~~ ~~the~~ continuous deepening. When these two phenomena meet, changes resulting from natural tectonic movements of a
363 riverbed may achieve equilibrium with time, whereas imbalance caused by anthropogenic structures may be enhanced with
364 time.

365 5. Conclusions

366 The Daan River, Zhoushui River, and Dajia River in central Taiwan exhibited changes in river morphology after
367 disturbance by earthquake uplift and dam obstruction during the past 20 years. The Daan River was affected by a thrust fault;
368 the Zhuoshui River was influenced by dam obstruction; and the Dajia River was both fault- and dam-influenced. In the Daan
369 River, the greater slope accelerated the flow velocity and drove knickpoint retreat after removal of the armor layer, resulting
370 in the progress of slope replacement. However, the incision faded with time, sediment deposition commenced, and the river
371 showed potential for recovery to a braided river pattern. Because of sediment trapping by the Jiji Dam, the Zhoushui River has

372 transformed from braided to gorge. The channelization started from the dam and expanded downward, and the incision progress
373 caused the local slope at the toe to become steeper. Because the dam acts as an immovable knickpoint, the river's sediment
374 equilibrium could not be re-established. The Shigang Dam on the Dajia River also caused a downward incision. The incision
375 from the toe of the dam subsequently connected with the knickpoint retreat caused by headward erosion from downstream,
376 forming a single, meandering channel at the front of the dam.

377 Knickpoints resulting from fault-induced riverbed uplift are moving points: as the knickpoint moves, the riverbed
378 evolves gradually from an unstable state to an equilibrium state. In contrast, a dam, as a fixpoint on the river, causes continuous
379 degradation. When both effects exist on a reach, the impact of the knickpoint gradually fades away, but the results of the dam
380 on the river persist.

381 **Author contribution**

382 The authors made the following contributions: HEC was involved in methods development, modeling, data analysis,
383 discussion, and paper preparation. YYC participated in data analysis, discussion, and paper preparation. CYC conducted the
384 field survey, collected and analyzed data. SCC contributed to [the preparation of](#) the hypothesis, concept, research design,
385 conclusions, and paper ~~preparation~~.

386 **Competing interests**

387 The authors declare that they have no conflict of interest.

388 **AcknowledgmentsAcknowledgements**

389 The Ministry of Science and Technology, Taiwan, partially supports this research under grant No. 111-2625-M-005-001.
390 The authors would like to thank AFASI, MOST, and CSRSR/NCU for supplying satellite imagery data and WRA for supplying
391 river measurement data.

392 References

- 393 Ahmed, M. F., Rogers, J. D., and Ismail, E. H.: Knickpoints along the upper Indus River, Pakistan: an exploratory survey of
394 geomorphic processes, *Swiss Journal of Geosciences*, 111, 191-204, <https://doi.org/10.1007/s00015-017-0290-3>, 2018.
- 395 [Alonso, C. V., Bennett, S. J., and Stein, O. R.: Predicting head-cut erosion and migration in concentrated flows typical of
396 upland areas, *Water Resources Research*, 38, 39-51, <https://doi.org/10.1029/2001wr001173>, 2002.](https://doi.org/10.1029/2001wr001173)
- 397 Bishop, P., Hoey, T. B., Jansen, J. D., and Artza, I. L.: Knickpoint recession rate and catchment area: the case of uplifted
398 rivers in Eastern Scotland, *Earth Surface Processes and Landforms*, 30, 767-778, <https://doi.org/10.1002/esp.1191>, 2005.
- 399 Braatne, J. H., Rood, S. B., Goater, L. A., and Blair, C. L.: Analyzing the impacts of dams on riparian ecosystems: a review
400 of research strategies and their relevance to the Snake River through Hells Canyon, *Environmental Management*, 41, 267-
401 281, <https://doi.org/10.1007/s00267-007-9048-4>, 2008.
- 402 Brandt, S. A.: Classification of geomorphological effects downstream of dams, *Catena*, 40, 375-401,
403 [https://doi.org/10.1016/S0341-8162\(00\)00093-X](https://doi.org/10.1016/S0341-8162(00)00093-X), 2000.
- 404 Bressan, F., Papanicolaou, A. N., and Abban, B.: A model for knickpoint migration in first- and second-order streams,
405 *Geophysical Research Letters*, 41, 4987-4996, <https://doi.org/10.1002/2014GL060823>, 2014.
- 406 Chamberlin, T. C., and Salisbury, R. D.: *Geology: Geologic processes and their results*, H. Holt, 1904.
- 407 Choi, S. U., Yoon, B., and Woo, H.: Effects of dam-induced flow regime change on downstream river morphology and
408 vegetation cover in the Hwang River, Korea, *River Research and Applications*, 21, 315-325, <https://doi.org/10.1002/tra.849>,
409 2005.
- 410 Clark, M. K., Maheo, G., Saleeby, J., and Farley, K. A.: The non-equilibrium landscape of the southern Sierra Nevada ,
411 California, 5173, [https://doi.org/10.1130/1052-5173\(2005\)15](https://doi.org/10.1130/1052-5173(2005)15), 2014.
- 412 Cook, K. L., Turowski, J. M., and Hovius, N.: A demonstration of the importance of bedload transport for fluvial bedrock
413 erosion and knickpoint propagation, *Earth Surface Processes and Landforms*, 38, 683-695, <https://doi.org/10.1002/esp.3313>,
414 2013.
- 415 Cook, K. L., Turowski, J. M., and Hovius, N.: River gorge eradication by downstream sweep erosion, *Nature Geoscience*, 7,
416 682-686, <https://doi.org/10.1038/ngeo2224>, 2014.
- 417 Crosby, B. T., and Whipple, K. X.: Knickpoint initiation and distribution within fluvial networks: 236 waterfalls in the
418 Waipaoa River, North Island, New Zealand, *Geomorphology*, 82, 16-38, <https://doi.org/10.1016/j.geomorph.2005.08.023>,
419 2006.
- 420 [Dotterweich, M.: The history of soil erosion and fluvial deposits in small catchments of central Europe: deciphering the
421 long-term interaction between humans and the environment—a review, *Geomorphology*, 101, 192–208,
422 <https://doi.org/10.1016/j.geomorph.2008.05.023>, 2008.](https://doi.org/10.1016/j.geomorph.2008.05.023)
- 423 Gardner, T. W.: Experimental study of knickpoint and longitudinal profile evolution in cohesive, homogeneous material,
424 *Geological Society of America Bulletin*, 94, 664-672, 1983.
- 425 Graf, W. L.: Downstream hydrologic and geomorphic effects of large dams on American rivers, *Geomorphology*, 79, 336-
426 360, <https://doi.org/10.1016/j.geomorph.2006.06.022>, 2006.
- 427 Hayakawa, Y. S., Matsuta, N., and Matsukura, Y.: Rapid recession of fault-scarp waterfalls: Six-year changes following the
428 921 Chi-Chi Earthquake in Taiwan, *Chikei/Transactions, Japanese Geomorphological Union*, 30, 1-13, 2009.
- 429 Heijnen, M. S., Clare, M. A., Cartigny, M. J. B., Talling, P. J., Hage, S., Lintern, D. G., Stacey, C., Parsons, D. R., Simmons,
430 S. M., Chen, Y., Sumner, E. J., Dix, J. K., and Hughes Clarke, J. E.: Rapidly-migrating and internally-generated knickpoints
431 can control submarine channel evolution, *Nature Communications*, 11, 3129-3129, [https://doi.org/10.1038/s41467-020-
16861-x](https://doi.org/10.1038/s41467-020-
432 16861-x), 2020.

433 [Hoffmann, T.: Sediment residence time and connectivity in non-equilibrium and transient geomorphic systems, Earth-](#)
434 [Science Rev., 150, 609–627, <https://doi.org/10.1016/j.earscirev.2015.07.008>, 2015.](#)

435 Holland, W. N., and Pickup, G.: Flume study of knickpoint development in stratified sediment, Geological Society of
436 America Bulletin, 87, 76-82, [https://doi.org/10.1130/0016-7606\(1976\)87<76:FSOKDI>2.0.CO;2](https://doi.org/10.1130/0016-7606(1976)87<76:FSOKDI>2.0.CO;2), 1976.

437 Horn, J. D., Joeckel, R. M., and Fielding, C. R.: Progressive abandonment and planform changes of the central Platte River
438 in Nebraska, central USA, over historical timeframes, Geomorphology, 139, 372-383,
439 <https://doi.org/10.1016/j.geomorph.2011.11.003>, 2012.

440 Howard, A. D., Dietrich, W. E., and Seidl, M. A.: Modeling fluvial erosion on regional to continental scales, Journal of
441 Geophysical Research, 99, <https://doi.org/10.1029/94jb00744>, 1994.

442 Huang, M.-W., Pan, Y.-W., and Liao, J.-J.: A case of rapid rock riverbed incision in a coseismic uplift reach and its
443 implications, Geomorphology, 184, 98-110, <https://doi.org/10.1016/j.geomorph.2012.11.022>, 2013.

444 Huang, M. W., Liao, J. J., Pan, Y. W., and Cheng, M. H.: Rapid channelization and incision into soft bedrock induced by
445 human activity - Implications from the Bachang River in Taiwan, Engineering Geology, 177, 10-24,
446 <https://doi.org/10.1016/j.enggeo.2014.05.002>, 2014.

447 Inbar, M.: EFFECT OF DAMS ON MOUNTAINOUS BEDROCK RIVERS, Physical Geography, 11, 305-319,
448 <https://doi.org/10.1080/02723646.1990.10642409>, 1990.

449 Kingsford, R. T.: Ecological impacts of dams, water diversions and river management on floodplain wetlands in Australia,
450 Austral Ecology, 25, 109-127, <https://doi.org/10.1046/j.1442-9993.2000.01036.x>, 2000.

451 Kong, D., Latrubesse, E. M., Miao, C., and Zhou, R.: Morphological response of the Lower Yellow River to the operation of
452 Xiaolangdi Dam, China, Geomorphology, 350, 106931-106931, <https://doi.org/10.1016/j.geomorph.2019.106931>, 2020.

453 Kuo, C.-W., Tfwala, S., Chen, S.-C., An, H.-P., and Chu, F.-Y.: Determining transition reaches between torrents and
454 downstream rivers using a valley morphology index in a mountainous landscape, Hydrological Processes, 35, e14393,
455 <https://doi.org/10.1002/hyp.14393>, 2021.

456 Lai, Y. G., Greimann, B. P., and Wu, K.: Soft Bedrock Erosion Modeling with a Two-Dimensional Depth-Averaged Model,
457 Journal of Hydraulic Engineering, 137, 804–814, [https://doi.org/10.1061/\(asce\)hy.1943-7900.0000363](https://doi.org/10.1061/(asce)hy.1943-7900.0000363), 2011.

458 [Lang, A., Bork, H., Mäckel, R., Preston, N., Wunderlich, J., and Dikau, R.: Changes in sediment flux and storage within a](#)
459 [fluvial system: some examples from the Rhine catchment, Hydrol. Process., 17, 3321–3334,](#)
460 <https://doi.org/10.1002/hyp.1389>, 2003.

461 Lee, J. C., Chu, H. T., Angelier, J., Chan, Y. C., Hu, J. C., Lu, C. Y., and Rau, R. J.: Geometry and structure of northern
462 surface ruptures of the 1999 Mw = 7.6 Chi-Chi Taiwan earthquake: Influence from inherited fold belt structures, Journal of
463 Structural Geology, 24, 173-192, [https://doi.org/10.1016/S0191-8141\(01\)00056-6](https://doi.org/10.1016/S0191-8141(01)00056-6), 2002.

464 Leopold, L. B. and Wolman, M. G.: River channel patterns: braided, meandering, and straight, US Government Printing
465 Office, 1957.

466 Lin, A., Ouchi, T., Chen, A., and Maruyama, T.: Co-seismic displacements, folding and shortening structures along the
467 Chelungpu surface rupture zone occurred during the 1999 Chi-Chi (Taiwan) earthquake, Tectonophysics, 330, 225-244,
468 [https://doi.org/10.1016/S0040-1951\(00\)00230-4](https://doi.org/10.1016/S0040-1951(00)00230-4), 2001.

469 Liro, M.: Dam-induced base-level rise effects on the gravel-bed channel planform, Catena, 153, 143-156,
470 <https://doi.org/10.1016/j.catena.2017.02.005>, 2017.

471 Liro, M.: Dam reservoir backwater as a field-scale laboratory of human-induced changes in river biogeomorphology: A
472 review focused on gravel-bed rivers, Science of the Total Environment, 651, 2899-2912,
473 <https://doi.org/10.1016/j.scitotenv.2018.10.138>, 2019.

474 Lyell Sir, C., and Deshayes, G. P.: Principles of geology; being an attempt to explain the former changes of the earth's
475 surface, by reference to causes now in operation, J. Murray, London, 1830.

476 Magilligan, F. J., and Nislow, K. H.: Changes in hydrologic regime by dams, *Geomorphology*, 71, 61-78,
477 <https://doi.org/10.1016/j.geomorph.2004.08.017>, 2005.

478 Merritts, D., and Vincent, K. R.: Geomorphic response of coastal streams to low, intermediate, and high rates of uplift,
479 Medocino triple junction region, northern California, *GSA Bulletin*, 101, 1373-1388, [https://doi.org/10.1130/0016-7606\(1989\)101<1373:GROCST>2.3.CO;2](https://doi.org/10.1130/0016-7606(1989)101<1373:GROCST>2.3.CO;2), 1989.

481 Miodrag, S., and M, H. F.: 2-D Bed Evolution in Natural Watercourses—New Simulation Approach, *Journal of Waterway,
482 Port, Coastal, and Ocean Engineering*, 116, 425-443, [https://doi.org/10.1061/\(ASCE\)0733-950X\(1990\)116:4\(425\)](https://doi.org/10.1061/(ASCE)0733-950X(1990)116:4(425)), 1990.

483 Nelson, N. C., Erwin, S. O., and Schmidt, J. C.: Spatial and temporal patterns in channel change on the Snake River
484 downstream from Jackson Lake dam, Wyoming, *Geomorphology*, 200, 132-142,
485 <https://doi.org/10.1016/j.geomorph.2013.03.019>, 2013.

486 Olsen, N. R. B.: Two-dimensional numerical modelling of flushing processes in water reservoirs, *Journal of Hydraulic
487 Research*, 37, 3-16, <https://doi.org/10.1080/00221689909498529>, 1999.

488 Ota, Y., Chen, Y.-G., and Chen, W.-S.: Review of paleoseismological and active fault studies in Taiwan in the light of the
489 Chichi earthquake of September 21, 1999, *Tectonophysics*, 408, 63-77, <https://doi.org/10.1016/j.tecto.2005.05.040>, 2005.

490 ~~Parker, G., and Izumi, N.: Purely erosional cyclic and solitary steps created by flow over a cohesive bed, *Journal of Fluid
491 Mechanics*, 419, 203-238, <https://doi.org/10.1017/S0022112000001403>, 2000.~~

492 Petts, G. E., and Gurnell, A. M.: Dams and geomorphology: research progress and future directions, *Geomorphology*, 71,
493 27-47, <https://doi.org/10.1016/j.geomorph.2004.02.015>, 2005.

494 Seidl, M. A., and Dietrich, W. E.: The problem of channel erosion into bedrock, *Functional geomorphology*, 101-124, 1992.

495 Shafroth, P. B., Perry, L. G., Rose, C. A., and Braatne, J. H.: Effects of dams and geomorphic context on riparian forests of
496 the Elwha River, Washington, *Ecosphere*, 7, e01621-e01621, <https://doi.org/10.1002/ecs2.1621>, 2016.

497 Słowik, M., Dezső, J., Marciniak, A., Tóth, G., and Kovács, J.: Evolution of river planforms downstream of dams: Effect of
498 dam construction or earlier human-induced changes?, *Earth Surface Processes and Landforms*, 43, 2045-2063,
499 <https://doi.org/10.1002/esp.4371>, 2018.

500 Surian, N., and Rinaldi, M.: Morphological response to river engineering and management in alluvial channels in Italy,
501 *Geomorphology*, 50, 307-326, [https://doi.org/10.1016/S0169-555X\(02\)00219-2](https://doi.org/10.1016/S0169-555X(02)00219-2), 2003.

502 Tomkin, J. H., Brandon, M. T., Pazzaglia, F. J., Barbour, J. R., and Willett, S. D.: Quantitative testing of bedrock incision
503 models for the Clearwater River, NW Washington State, *Journal of Geophysical Research: Solid Earth*, 108,
504 <https://doi.org/10.1029/2001jb000862>, 2003.

505 Whipple, K. X., and Tucker, G. E.: Dynamics of the stream-power river incision model: Implications for height limits of
506 mountain ranges, landscape response timescales, and research needs, *Journal of Geophysical Research: Solid Earth*, 104,
507 17661-17674, <https://doi.org/10.1029/1999jb900120>, 1999.

508 Whipple, K. X.: Fluvial landscape response time: how plausible is steady-state denudation?, *American Journal of Science*,
509 301, 313-325, <https://doi.org/10.2475/ajs.301.4-5.313>, 2001.

510 Whipple, K. X., and Tucker, G. E.: Implications of sediment-flux-dependent river incision models for landscape evolution,
511 *Journal of Geophysical Research: Solid Earth*, 107, ETG 3-1-ETG 3-20, doi.org/10.1029/2000JB000044, 2002.

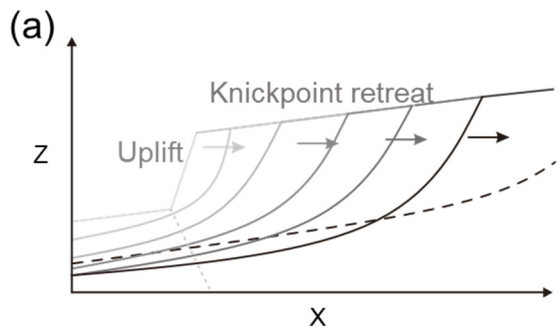
512 Whipple, K. X.: BEDROCK RIVERS AND THE GEOMORPHOLOGY OF ACTIVE OROGENS, *Annual Review of Earth
513 and Planetary Sciences*, 32, 151-185, <https://doi.org/10.1146/annurev.earth.32.101802.120356>, 2004.

514 Williams, G. P., and Wolman, M. G.: Downstream effects of dams on alluvial rivers 1286, 1984.

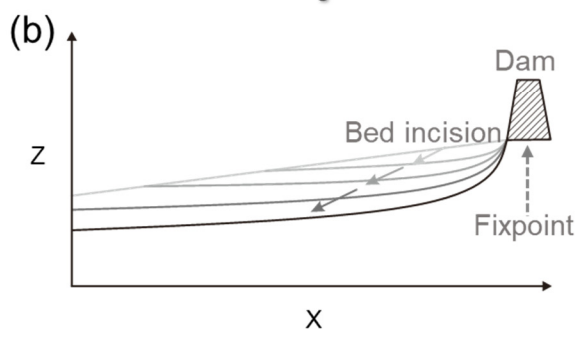
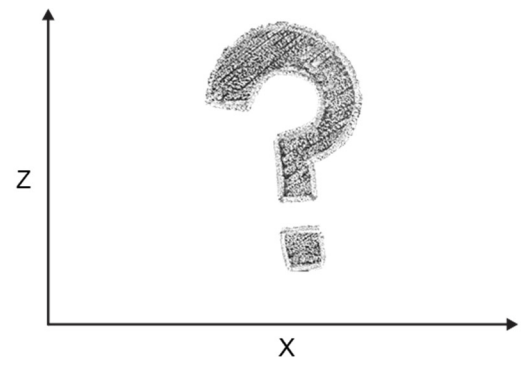
515 Zhou, M., Xia, J., Deng, S., Lu, J., and Lin, F.: Channel adjustments in a gravel-sand bed reach owing to upstream damming,
516 *Global and Planetary Change*, 170, 213-220, <https://doi.org/10.1016/j.gloplacha.2018.08.014>, 2018.
517
518

Table 1 Characteristics of the studied reaches of the Daan, Zhuoshui, and Dajia rivers

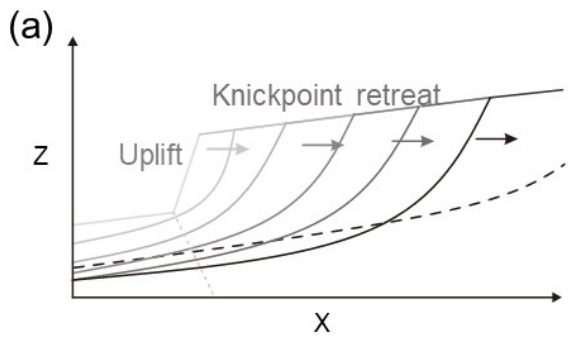
River	Time interval	Section	Bed Change		Channel Widening		Knickpoint retreat		C (m yr ⁻¹)	
			(m)	(m yr ⁻¹)	(m)	(m yr ⁻¹)	(m)	(m yr ⁻¹)		
Daan	2000–2004	a	-0.60	-0.15	-103.77	-25.94	85	21.25	22	
		b	-1.76	-0.44	47.50	11.88				
	2004–2007	a	-16.67	-5.56	-316.50	-105.50	422	140.67		
		b	-6.20	-2.07	-269.82	-89.94				
	2007–2011	a	2.06	0.52	19.30	4.83	412	103.00		
		b	-7.11	-1.78	-64.19	-16.05				
	2011–2016	a	-0.45	-0.09	31.19	6.24	--	--		
		b	-0.84	-0.17	41.27	8.25	--	--		
	Zhuoshui	1998–2008	c	-0.46	-0.05	-96.22	-9.62	--		--
			d	-2.24	-0.22	-130.41	-13.04			
e			-11.59	-1.16	-246.32	-24.63				
2008–2012		c	-5.44	-1.36	-258.44	-64.61	--	--		
		d	-2.77	-0.69	18.43	4.61				
		e	3.00	0.75	5.22	1.31				
2012–2015		c	-4.46	-1.49	-171.56	-57.19	--	--		
		d	-6.65	-2.22	-133.24	-44.41				
		e	-4.94	-1.65	-73.11	-24.37				
2015–2018		c	-0.84	-0.28	13.57	4.52	--	--		
		d	-0.86	-0.29	1.31	0.44				
		e	-3.03	-1.01	8.70	2.90				
Dajia		2000–2005	f	-2.39	-0.48	-14.12	-2.82	40	8.00	7.5
			g	-2.02	-0.40	-116.44	-23.29			
		2005–2008	f	-2.57	-0.86	-39.90	-13.30	186	62.00	
	g		-7.50	-2.50	-142.97	-47.66				
	2008–2014	f	-1.33	-0.22	12.28	2.05	219	24.33		
		g	-0.38	-0.06	2.21	0.37				
	2010–2014	h	-4.20	-1.05	-25.45	-6.36				
	2014–2017	f	-1.39	-0.46	-10.44	-3.48				
		g	-3.32	-1.11	8.84	2.95				
		h	-5.27	-1.76	-20.63	-6.88				



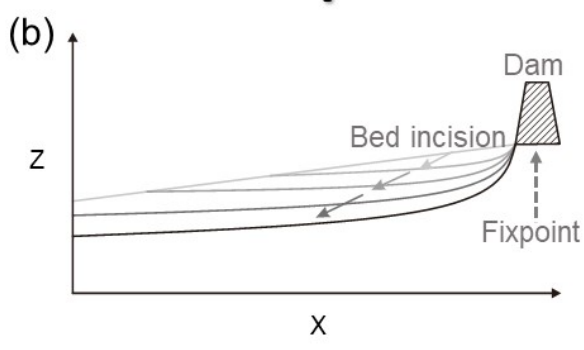
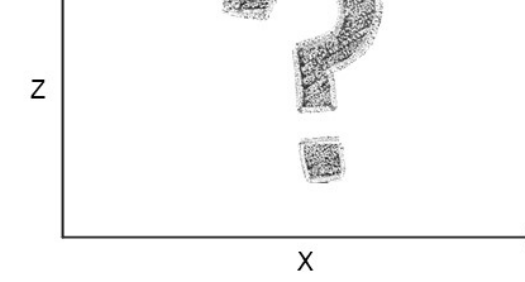
(c) How will the combined effects develop longitudinal profile?



521

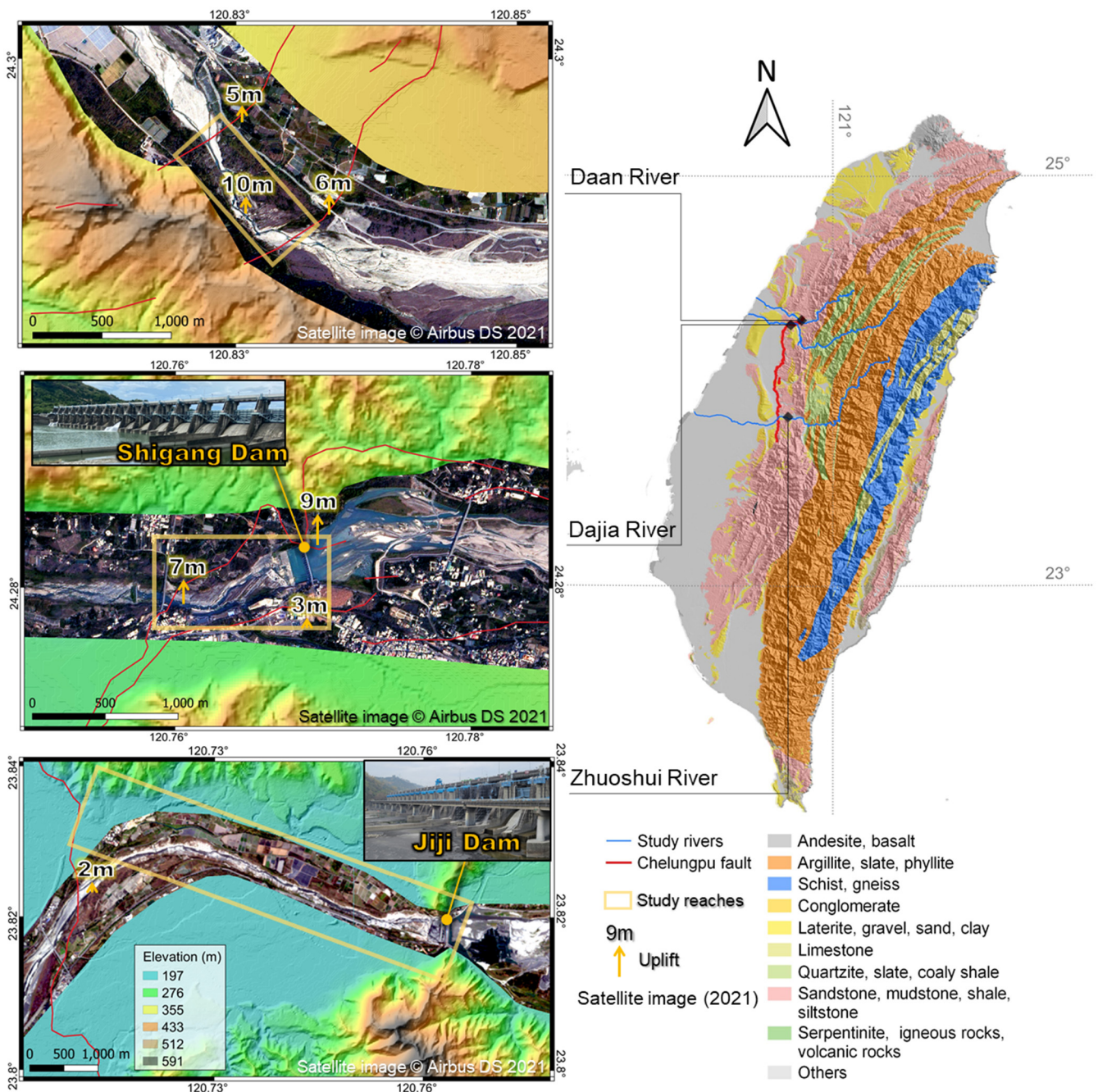


(c) How will the combined effects develop longitudinal profile?



522

523 Figure 1: Schematic diagrams of longitudinal profile development for (a) fault scarp's knickpoint, (b) dam's fixpoint,
 524 and (c) How will the combined effects develop longitudinal profile?

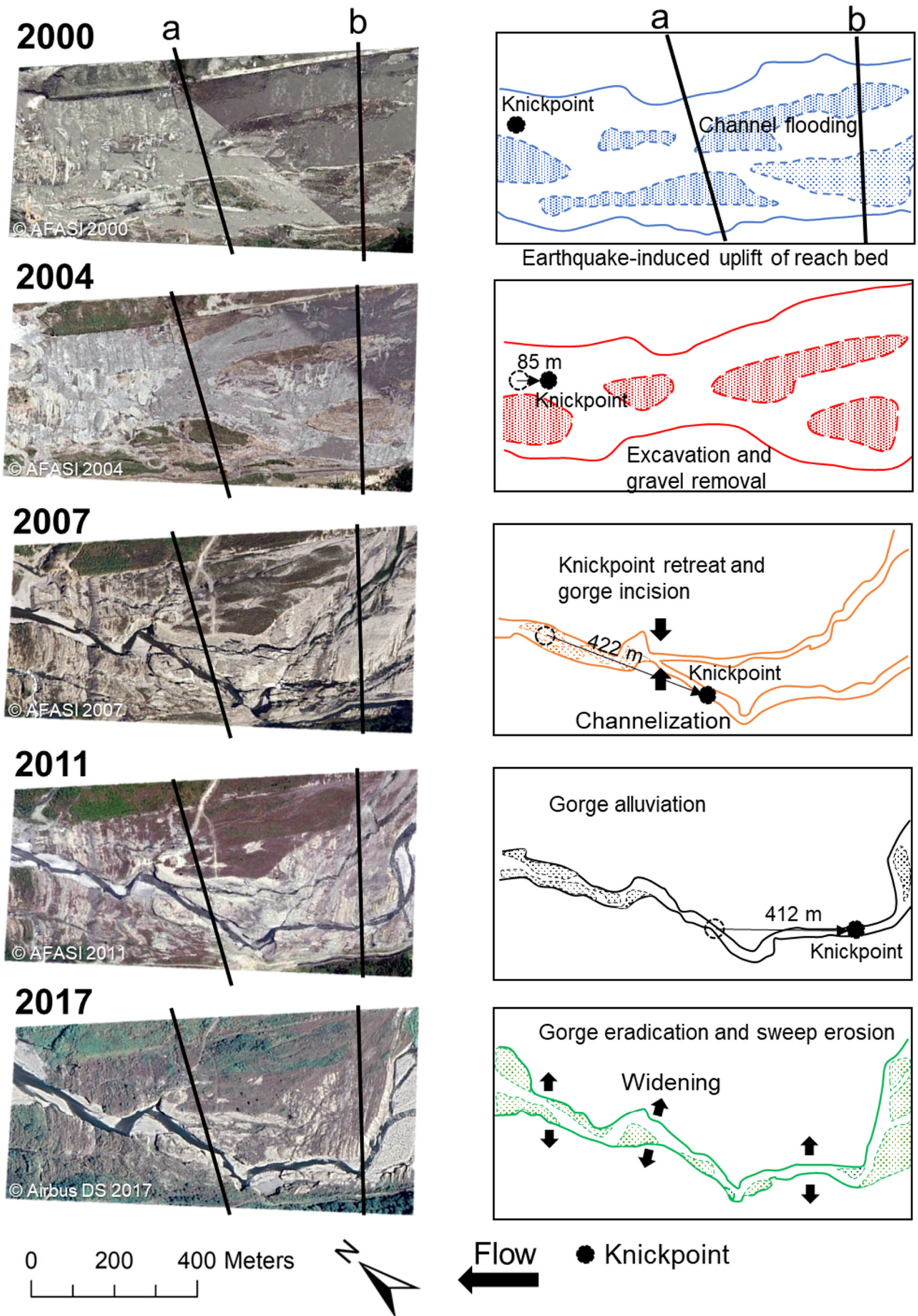


525

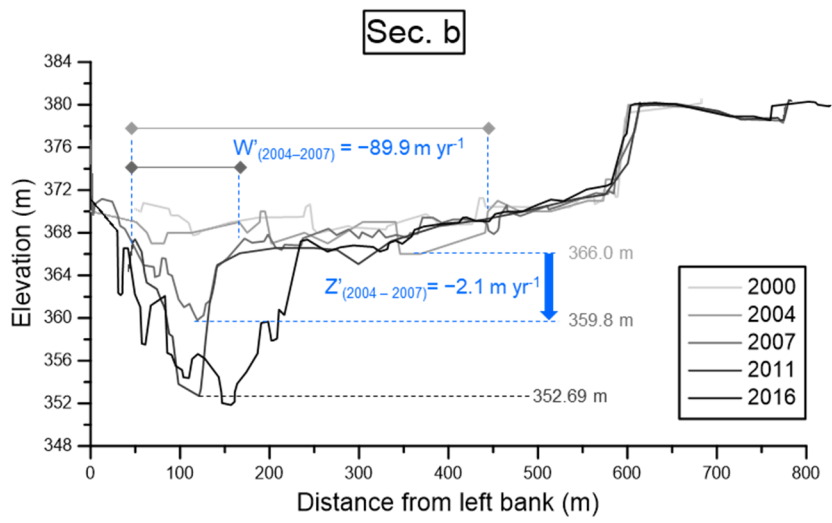
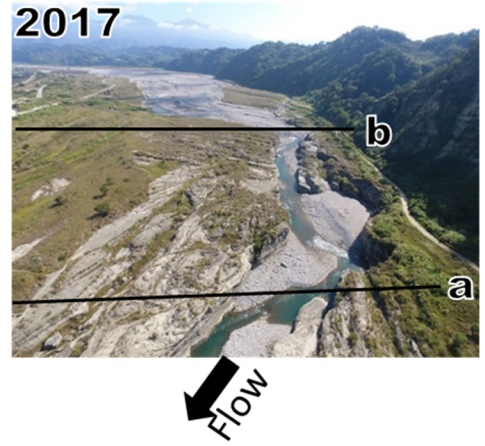
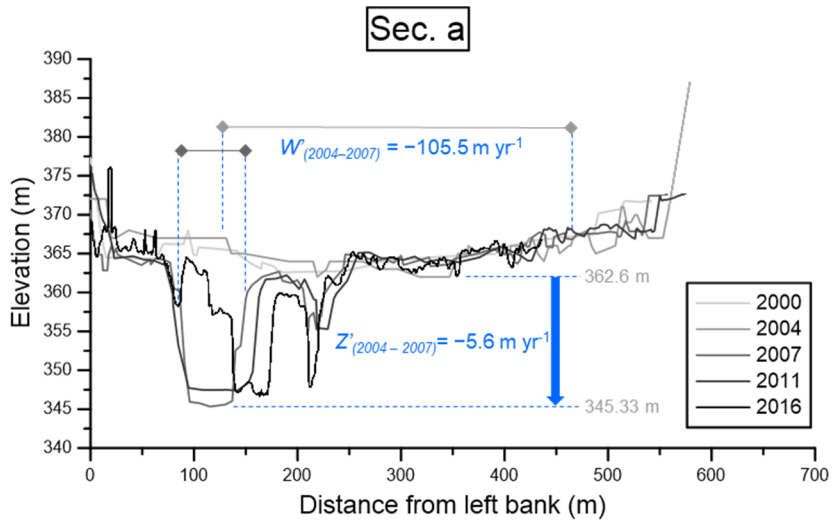
526

527

Figure 2: Locations of the Chelungpu Fault, the three studied rivers, and satellite images (from CSRSR/NCU date: 05-Feb-2021, 2m resolutions) showing the studied reaches.



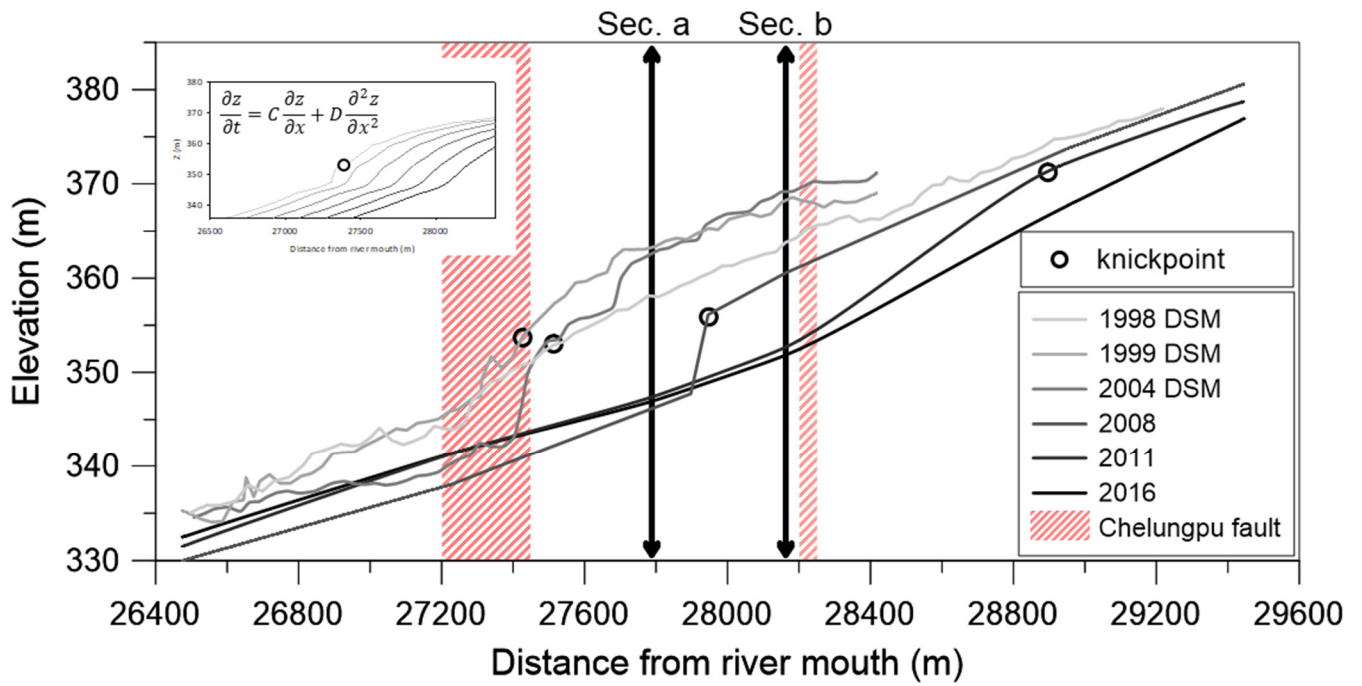
528
 529 **Figure 3: Orthographic images (2000–2011), satellite image (2017) and flow paths of the studied reach of the Daan**
 530 **River from 2000 to 2017.**



531

532 **Figure 4: Cross-sections a and b of the Daan River from 2000 to 2016 (from WRA).**

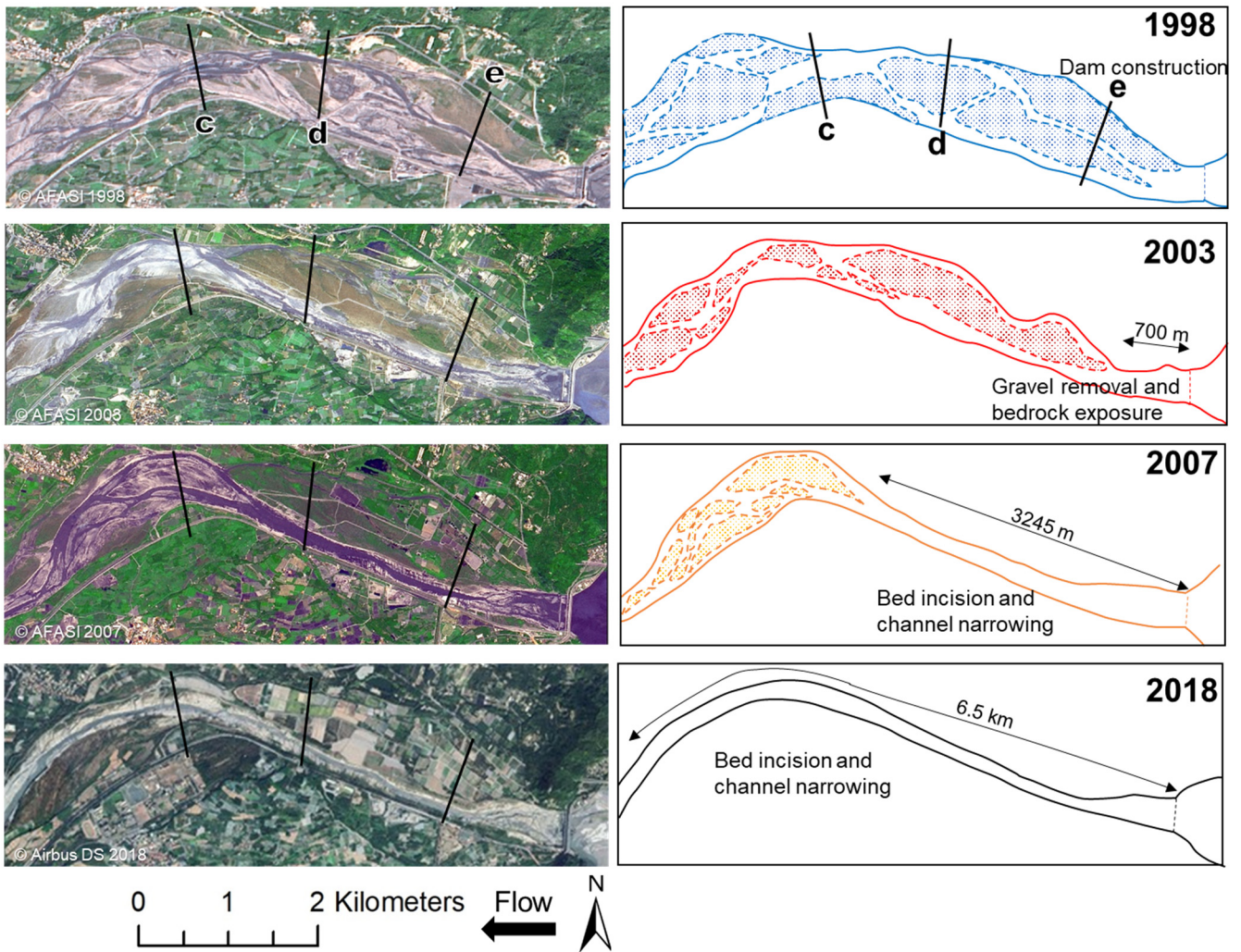
533



535

536 Figure 5: Longitudinal profiles of the studied reach of the Daan River from 2000 to 2016. Profiles for 1998–2008 are
 537 from Cook et al. (2013), and 2011–2016 are from WRA. Data between 1998 and 2004 are derived from aerial photograph
 538 generated Digital Surface Models (DSMs). The subfigure shows the simulated knickpoint retreats are
 539 simulated using the advective-diffusive model at the top left.

540

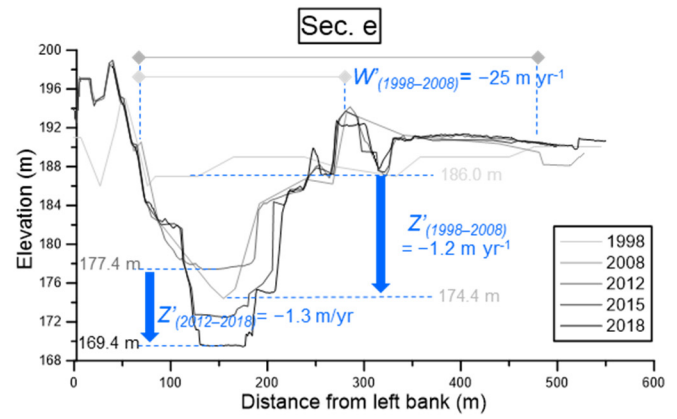
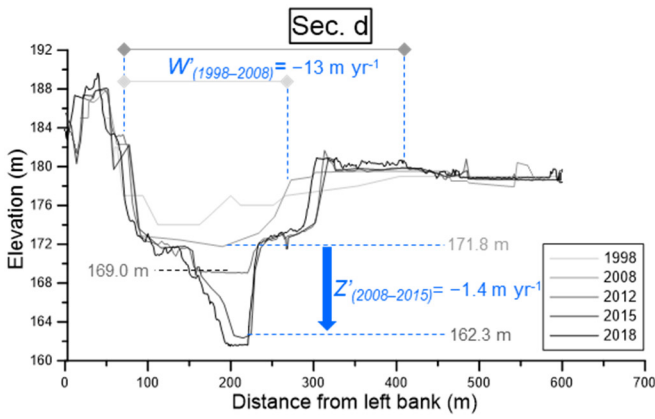
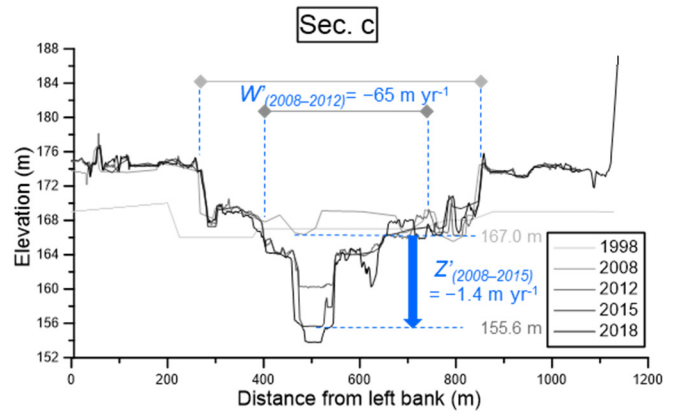
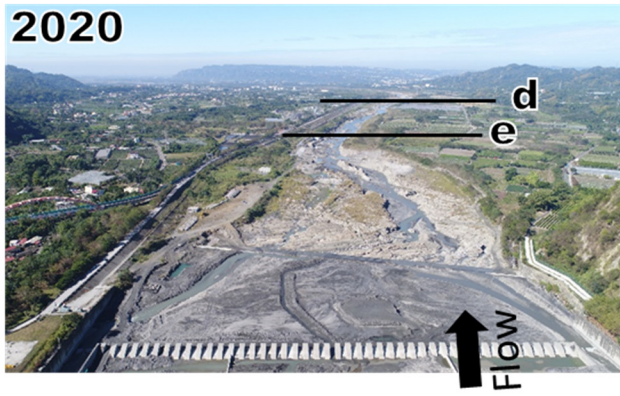


541

542 Figure 6: Orthographic images (1998–2007), satellite image (2018), and flow paths of the studied reach of the Zhuoshui

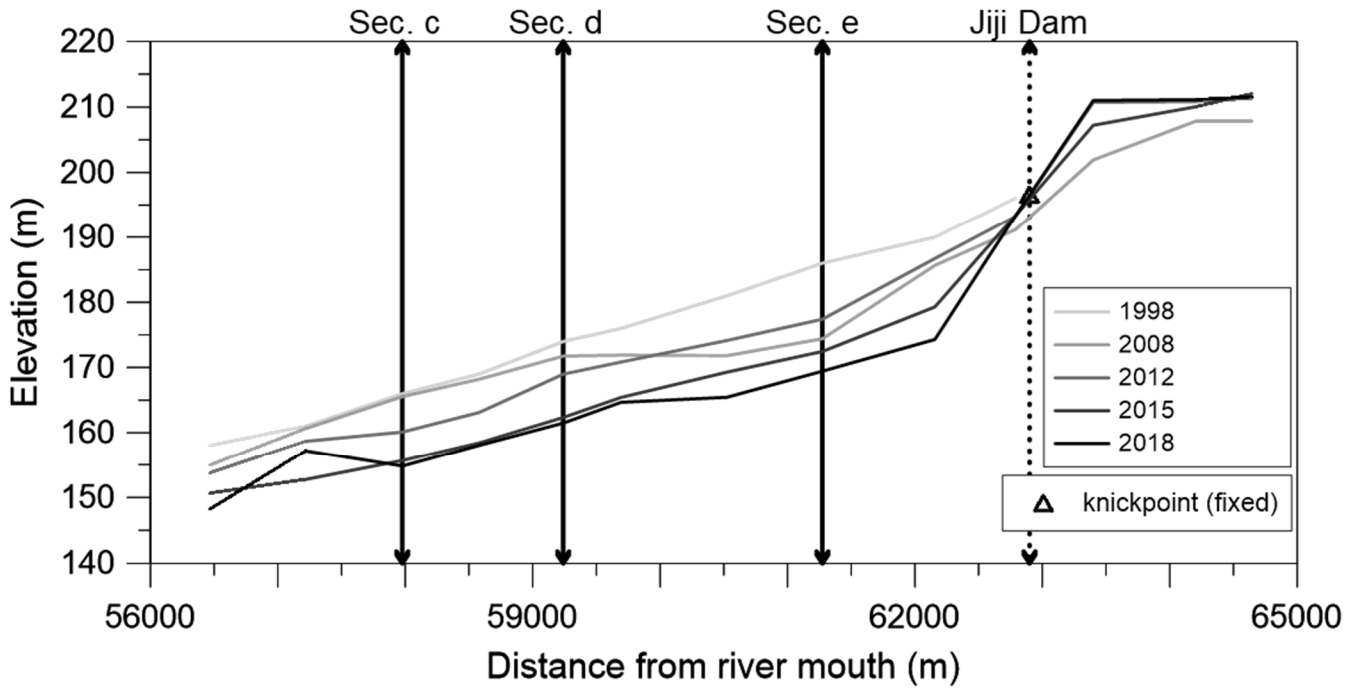
543 River from 1998 to 2018.

544

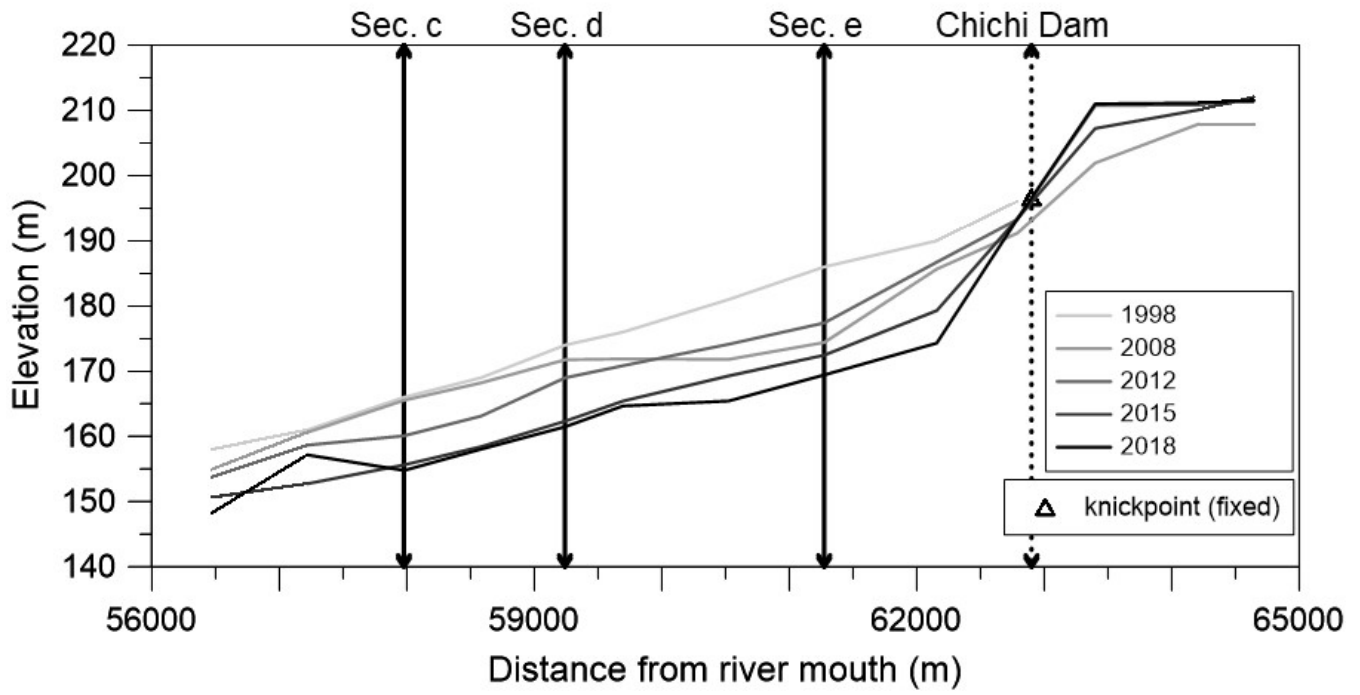


545
546

Figure 7: Profiles of cross-sections c, d, and e of the Zhuoshui River from 1998 to 2018 (from WRA).



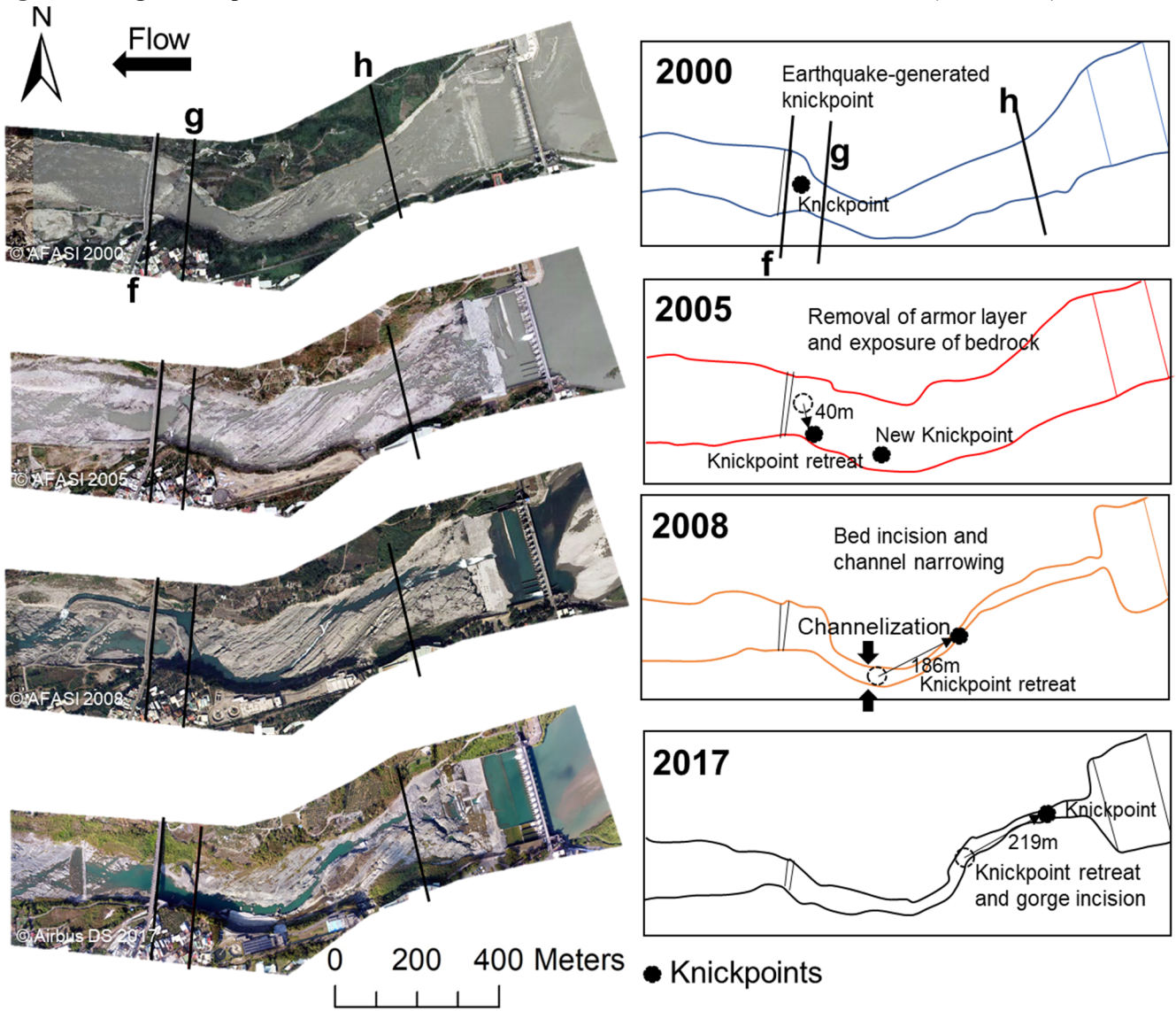
547



548

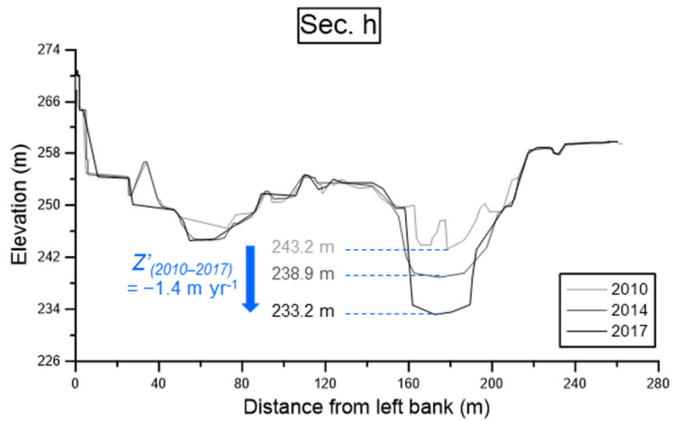
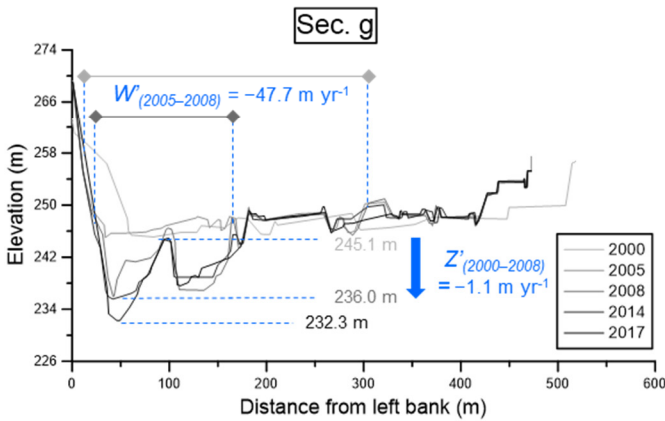
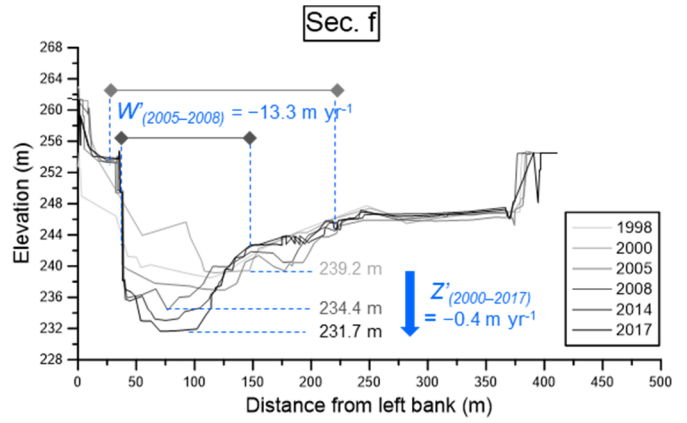
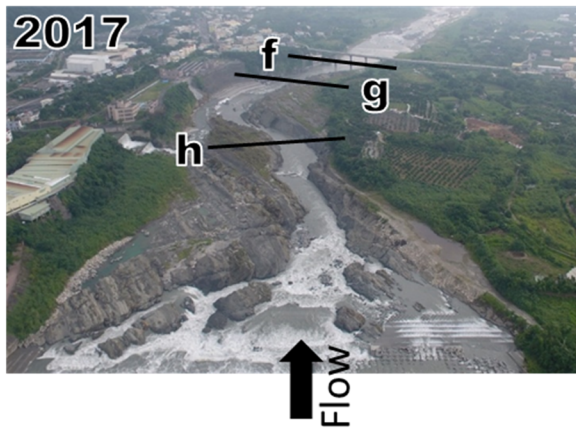
549

Figure 8: Longitudinal profiles of the studied reach of the Zhuoshui River from 1998 to 2018 (from WRA).

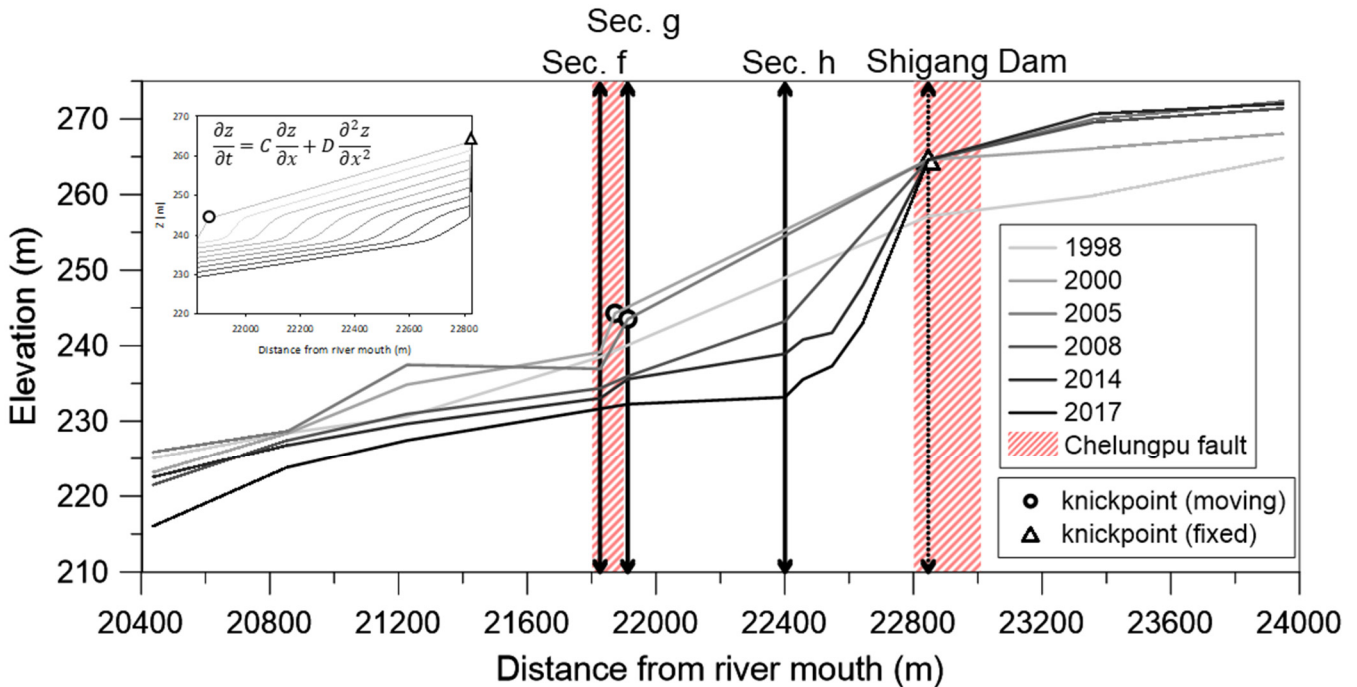


550

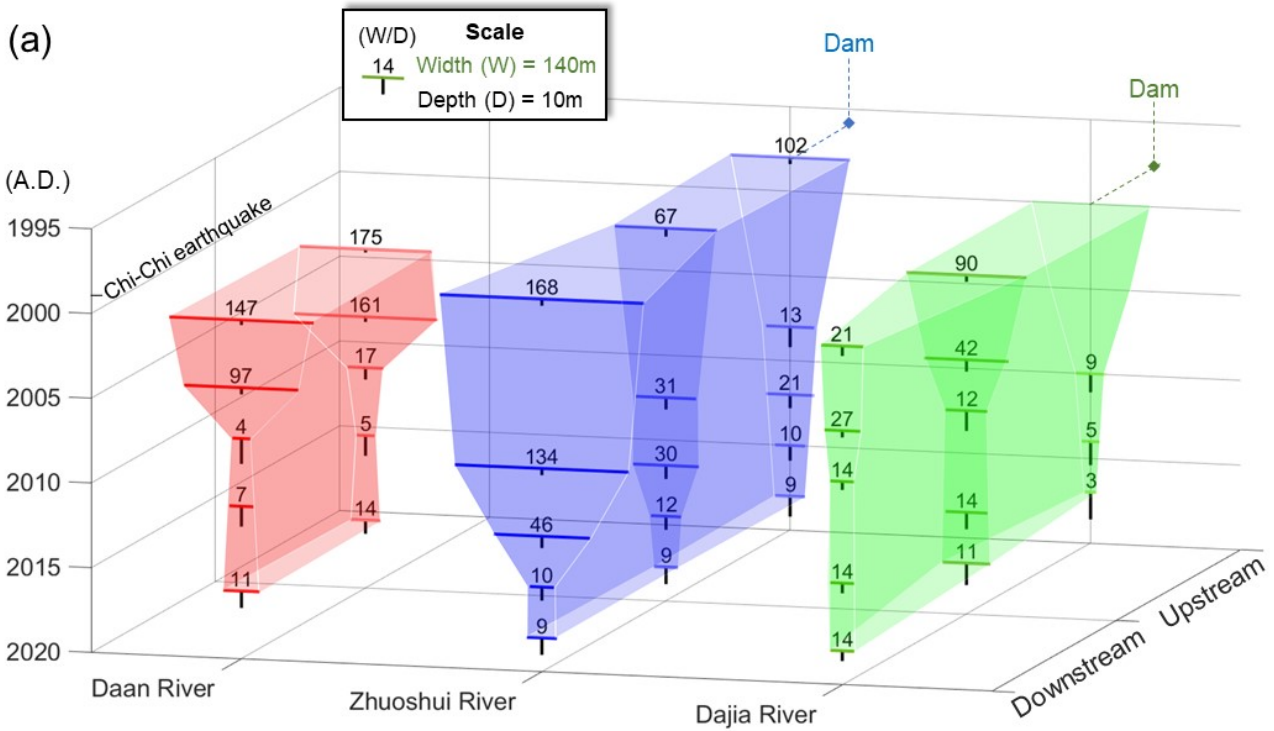
551 Figure 9: Orthographic images (2000–2008), satellite image (2017), and flow paths of the studied reach of the Dajia
 552 River from 2000 to 2017.



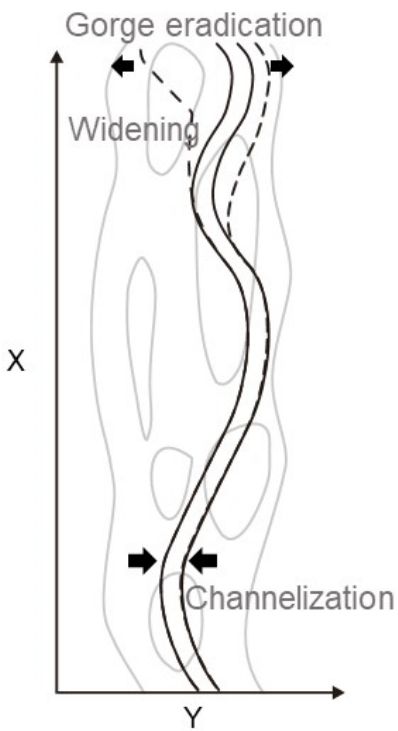
553
 554 Figure 10: Cross-sections f, g, and h of the Dajia River from 2000 to 2017 (from WRA).



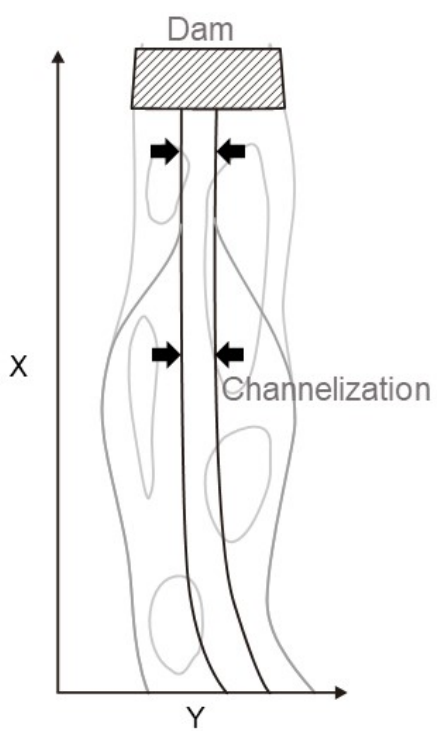
555
 556 Figure 11: Longitudinal profiles of the studied reach of the Dajia River from 1998 to 2017 (from WRA). Knickpoint
 557 retreats are simulated using the advective-diffusive model at the top left.
 558



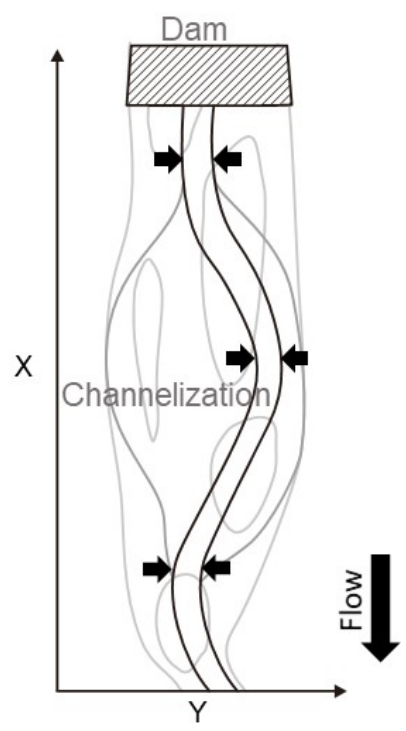
(b) Daan river



(c) Zhuoshui river



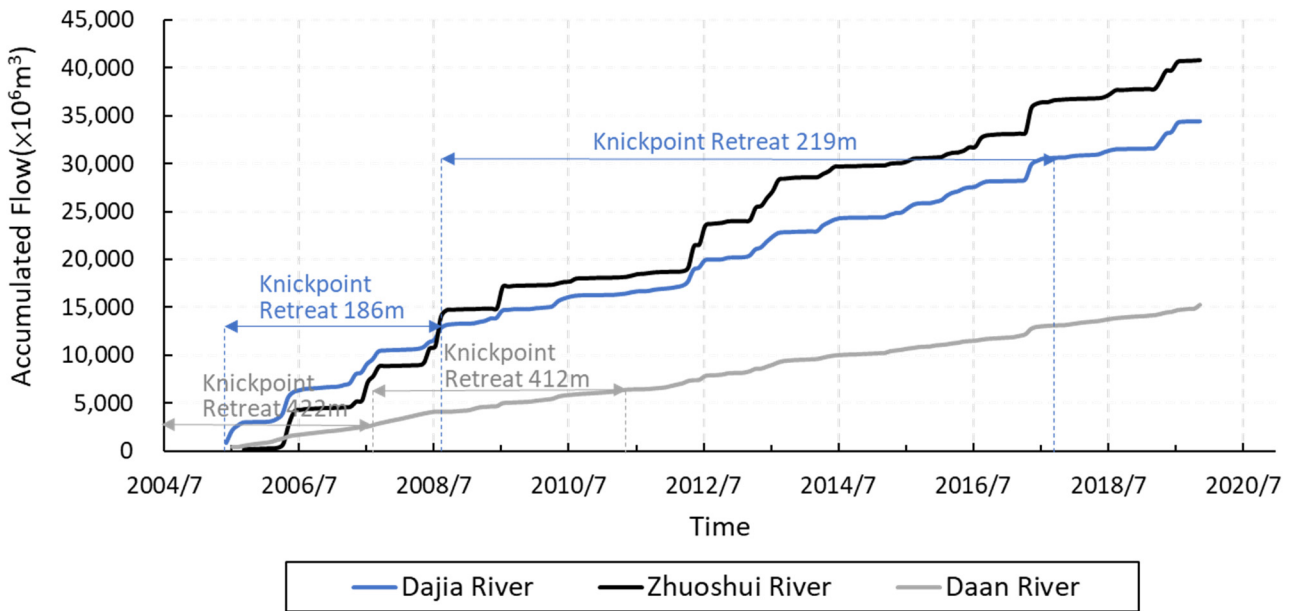
(d) Dajia river



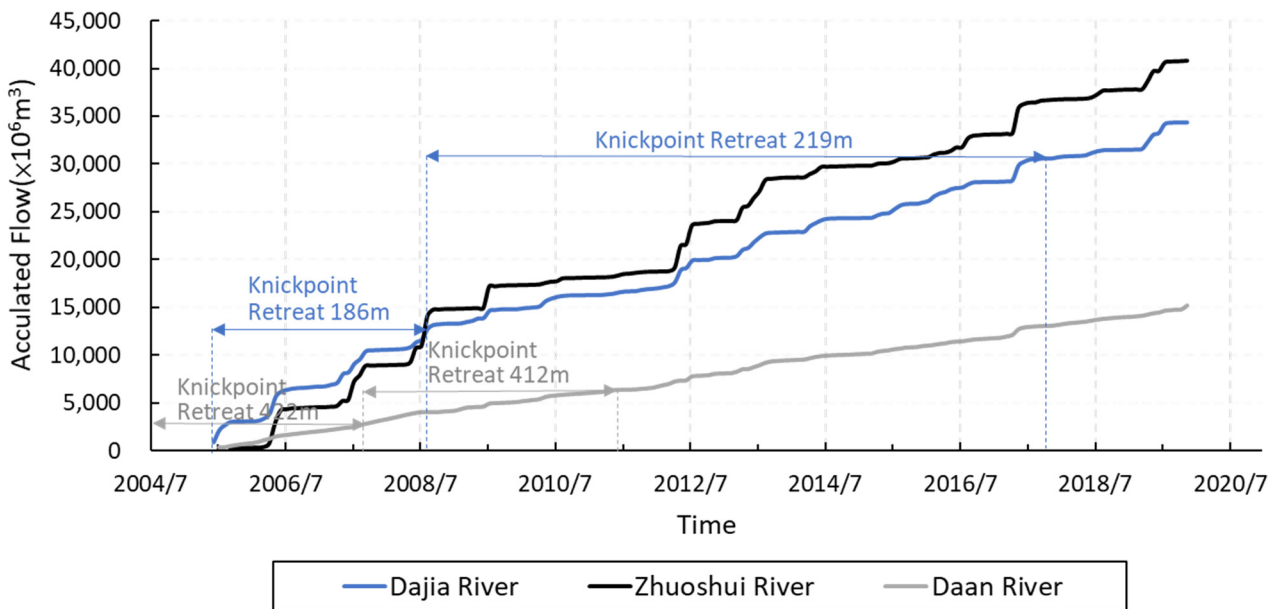
559

560

561 Figure 12: (a) Channel width (W), depth (D), and aspect ratio (W/D) of the studied reaches of the three rivers. The
 562 aspect ratio was defined as the ratio of the bankfull width to the depth of the bankfull channel. The vertical axis shows
 563 the time from 1995 downward to 2020, the horizontal axis shows the rivers, and the normal axis shows the sections
 564 from downstream to upstream. Schematic diagrams of knickpoint retreat and river pattern development for (b)
 565 coseismic uplift, (c) dam obstruction, and (d) dam obstruction and coseismic uplift.



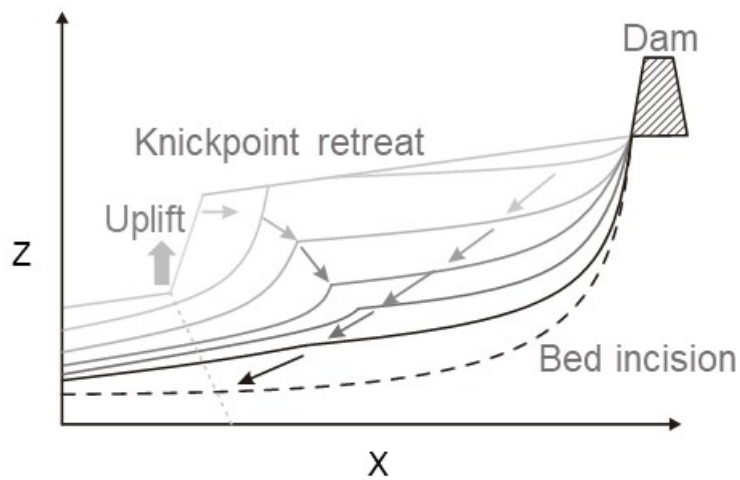
566



567

568

Figure 13: The cumulative flow in the three study reaches and the corresponding knickpoint retreat distances.



569

570 **Figure 14: A Schematic diagram of longitudinal profile development for the combined effects from dam construction**
571 **and coseismic uplift.**
572
573